Modeling Water Column and Benthic Effects of Fish Mariculture of Cobia (*Rachycentron canadum*) in Puerto Rico: Cobia AquaModel

Prepared for

Ocean Harvest Aquaculture Inc., Puerto Rico

and

The National Oceanic and Atmospheric Administration, Washington D.C.

By

Systems Science Applications, Inc.

P.O. Box 1589
Pacific Palisades, CA 90272
kiefer@runeasy.com
+1 (310) 678-5081

Dale A. Kiefer, Ph.D.
Frank O'Brien
J.E. Jack Rensel, Ph.D.

Irvine Ca.

FINAL REPORT

Table of Content

List of Figures

List of Tables

This report was prepared in part with funding from the National Oceanic and Atmospheric Administration and Ocean Harvest Aquaculture Inc. Because the report was prepared in part with public funds, this report is available to the public without reservation.

1. Executive Summary

This document is an analysis of potential water column and benthic cumulative effects of a proposed offshore, submerged fish farm to be located off the east coast of Puerto Rico. Ten individual, submerged SeaStation cages would be used to rear about 900,000 pounds (405MT) of cobia (*Rachycentron canadum).* The fish has an extraordinarily-fast growth rate and reaches a size of 5 kg about 9 months after hatch. This feature and other characteristics make cobia a excellent farmed-fish candidate.

The proposed fish culture area may be characterized as exposed, well-flushed coastal shelf remote from sensitive habitats such as coral reefs. Extensive current meter, acoustic Doppler current profiler and other studies have been conducted in preparation for the fish farm.

A proprietary modeling program known as AquaModel was used to simulate water and sediment quality effects of the proposed fish farm. It is the first comprehensive model for net-pen aquaculture that simultaneously accounts for both water column (dissolved oxygen, nitrogen, plankton) and benthic (particulate carbon sedimentation) effects.

AquaModel is composed of interlinked submodels of fish physiology, hydrodynamics, water quality, solids dispersion and assimilation. The system provides the user a 3-dimensional simulation of growth, metabolic activity of caged fish, associated flow and transformation of nutrients, oxygen, and particulate wastes in adjacent waters and sediments. AquaModel resides within a Geographic Information System (GIS) program designed for oceanographic use but is compatible with other common 2-dimensional GIS software.

The results of the modeling work indicated that relatively minor amounts of carbon will be deposited on the sea floor immediately under and near the cages. Mean current velocity at the site is relatively modest (about 10 cm s^{-1}) but current direction is highly variable and peak current velocity reaches ~ 50 cm s^{-1} (1 knot) affording a great deal of dispersion of particulate and dissolved wastes. These organic and inorganic wastes are not merely diluted, but are readily available for uptake and growth of marine invertebrates, fish and plankton. Many regulatory jurisdictions worldwide have decided this is the best means to manage marine fish farms, i.e., proper siting and avoidance of habitats of special significance in the immediate vicinity.

AquaModel applied to site specific conditions in Puerto Rico predicts levels of carbon-containing particulate wastes that may be easily assimilated by the benthic ecosystem. Current velocity is great enough to facilitate regular resuspension and aeration of the particulate matter, so that anaerobic conditions experienced under fish farms that were poorly sited in the past may be avoided. Perturbations of the water column will include slight reduction in dissolved oxygen in and very near the fish cages and slightly elevated dissolved nitrogen concentrations within the cages. The probability of stimulating a plankton bloom was shown to be essentially none, as phytoplankton cells have population doubling rates that are slow (days) compared to the advective properties of the site. In every case we used conservative to very conservative model calibration coefficients or constants to purposely investigate worst-possible-case conditions and to offset any limitations or inaccuracies of the model.

2. Introduction

2.1 Objectives, purpose and origin of model

The purpose of this report is document the use of an existing model called AquaModel that has been adapted to simulate the water column and benthic effects of an offshore fish farm proposed for the east coast of Puerto Rico. The fish farm is to be operated by Ocean Harvest Aquaculture Inc. of Puerto Rico and has been the focus of a number of studies, documents and reports referenced herein.

Our model is a composite of a pre-existing water column model first developed by Professor Dale Kiefer of the University of Southern California and his colleagues and a more recently developed benthic model that is similar to a widely used and published model developed in Scotland by the Scottish Marine Biological Association. The model was written in visual basic and operates with the Windows PC operating system. Dr. Kiefer and his co-workers including Dr. Jack Rensel have been involved in modeling aquaculture effects periodically since 1990 (Kiefer and Atkinson, 1988, 1989, Rensel 1987, 1989a, 1989b).

The model described herein is intended for use in simulating commercial fish farms operated as net pens in relatively well-flushed inshore or continental coastal-shelf waters sometimes referred to as "offshore aquaculture". The first application of the model simulated the water column effects of salmon farming in a high velocity tidal strait in the Pacific Northwest, in work performed for NOAA and the Washington Fish Growers Association. See http://www.wfga.net/sjdf/index.html and Rensel et al. (in press a). This version of the model faithfully reproduced the well-known and carefully documented physiological effects of salmon including their respiration (oxygen consumption), nitrogen excretion (mostly ammonia and minor amounts of urea that both rapidly convert to nitrate in the environment), microalgal (phytoplankton growth) resulting from the nitrogen excretion and zooplankton grazing upon the available stocks of phytoplankton in the modeling domain.

Subsequently, AquaModel has been expanded to include simulation of discharge and flux of carbon-containing solids from fish feces and waste feed that sink at known rates toward the bottom, are deposited upon surficial sediments and resuspended and re-transported laterally when near bottom current velocities exceed threshold values. The benthic submodel is patterned after the proprietary program known as DEPOMOD (Cromey et al. 2002a, 2002b) which in turn was derived in part from the well-known G-model of carbon degradation (Westrich and Berneir 1984) and subsequent studies described herein.

AquaModel may be classified as a 3-D multibox model with simplified hydrodynamic flows that allows use of real current meter data or simulated tidal flows based on site specific characteristics. AquaModel was not developed for broad use by other users as it runs within Geographic Information System software known as Environmental Analysis System (EASy) which has multiple and complex functions and purposes. At present the model is a consulting tool of Science Systems Applications (SSA) which is owned by Dr. Dale Kiefer and Mr. Frank O'brien. Dr. Jack

Rensel is an aquaculture effects specialist who works with SSA on model design, testing and application.

3. Detailed Model Description

To our knowledge our EASy AquaModel is the only software that provides a complete, dynamic model of farm operation and environmental impact. It is also the only software that fully integrates environmental information with model computations within a GIS. A simplified simulation of the water column portion of the model can be viewed via the Internet at http://netviewer.usc.edu/mariculture (use Internet Explorer and closely follow browser options). Our model and GIS system has the capability to contain environmental information obtained from satellite-ocean thermal and color sensors and field surveys of currents, nutrients, oxygen, and chlorophyll. It also contains a simulation of virtual farms that can be "placed" within a given water body and operated according to the conditions found at that location. Most importantly, the information system fully integrates field surveys of conditions in the water body with a dynamic model describing the growth and physiology of penned fish under any operating conditions selected by the user.

AquaModel was written in Visual Basic and coupled to the marine GIS software called EASy (Environmental Analysis System). The GIS software, which has been developed by our company SSA, provides a 4 dimensional framework (latitude, longitude, depth, and time) to run simulation models and analyze field measurements as graphical and statistical outputs. EASy, whose components are shown in figure 1, is an advanced, PC-based geographical information system designed for the storage, dissemination integration, analysis and dynamic display, of spatially referenced series of diverse oceanographic data.

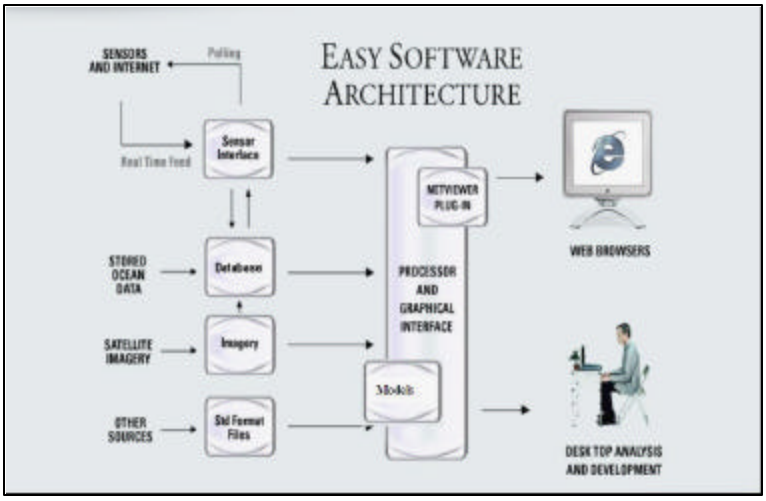

Figure 1. EASy software architecture and data integration

AquaModel graphically renders dynamically in time, within their proper geo-spatial context, both field and remotely sensed data and model outputs as diverse types of plots, including vector, contour, and false color images. Vertical structure of data, critical in oceanographic applications, is depicted as vertical contours for transects or depth profiles at selected point locations. Time series for measurements and relationships such as vertical profiles within the database at individual stations can also be visualized interactively as XY-plots. The software also provides

access to data, integrated visualization products, and analytical tools over the Internet via Netviewer, a client-server, plug-in for EASy. For more information and examples of real-world applications visit http://www.runeasy.com.

AquaModel, which is a computation module that couples to EASy, consists of 4 components: a 3 dimensional description of circulation, a description of the growth and metabolic activity of salmon within the farm, a description of the planktonic community's response to nutrient loading, and a description of the organic loading of carbon-containing sediments (Figure 2).

Parameters of the model, including pen array center, location in the Cartesian coordinate system, cell (grid) size, farm dimensions, capture cell locations (i.e., vertical profiles from specific locations that is exported to spreadsheets), fish loading and feed rates, etc., are set interactively with drop down menu selection (See Figure 2).

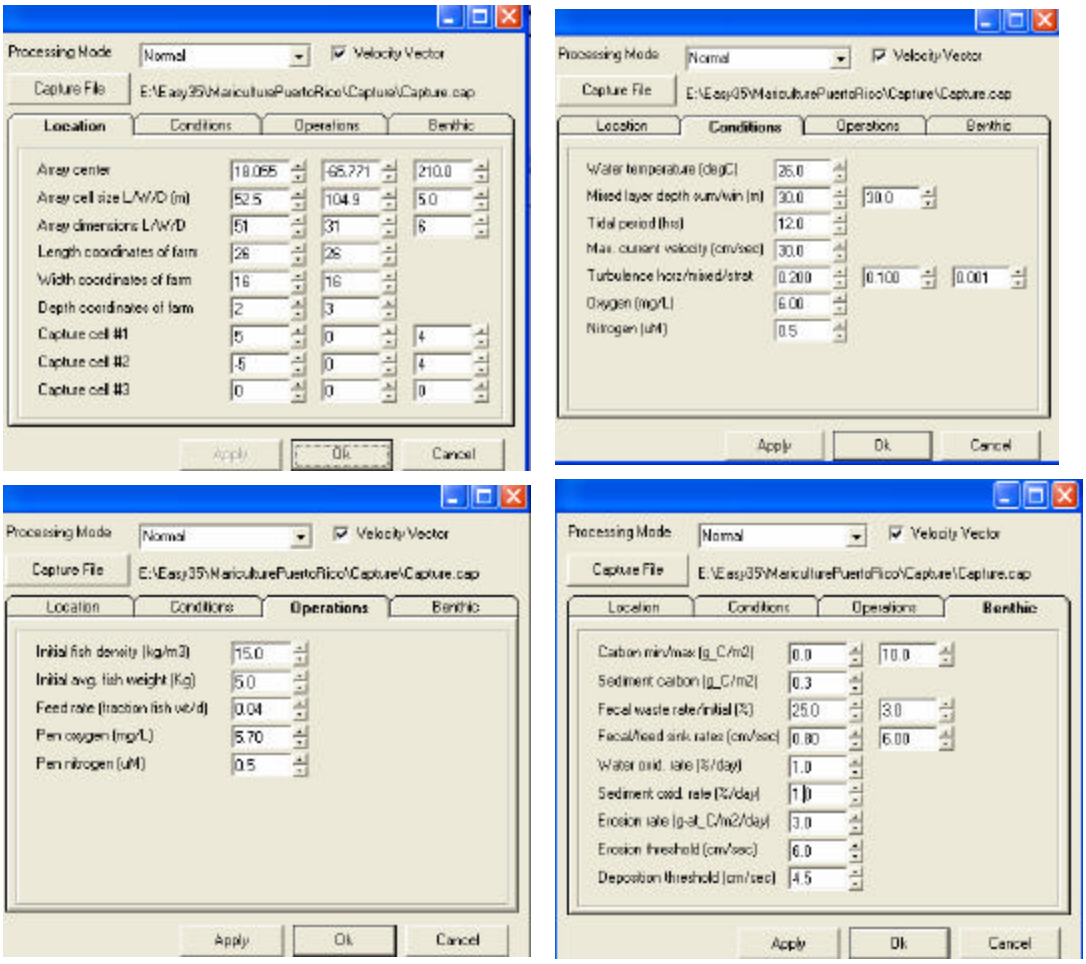

Figure 2. User settings of AquaModel Mariculture Options Panel.

from left to right, top to bottom: location, conditions, operations and benthic.

As indicated in Figure 3, the system of equations that characterize the dynamics of the planktonic community traces the cycling of carbon, nitrogen, and oxygen within each element of the array, both within the farm and the surrounding waters, and output from the model (Kiefer & Atkinson,

1984). Outputs consist of the time series at each element of the array of the concentrations of dissolved inorganic nitrogen, carbon dioxide, and oxygen, as well as the organic nitrogen and carbon in the phytoplankton, and zooplankton. The model displays predator-prey oscillations that dampen with time, reaching a steady state. Next we describe the model by submodel components in more detail.

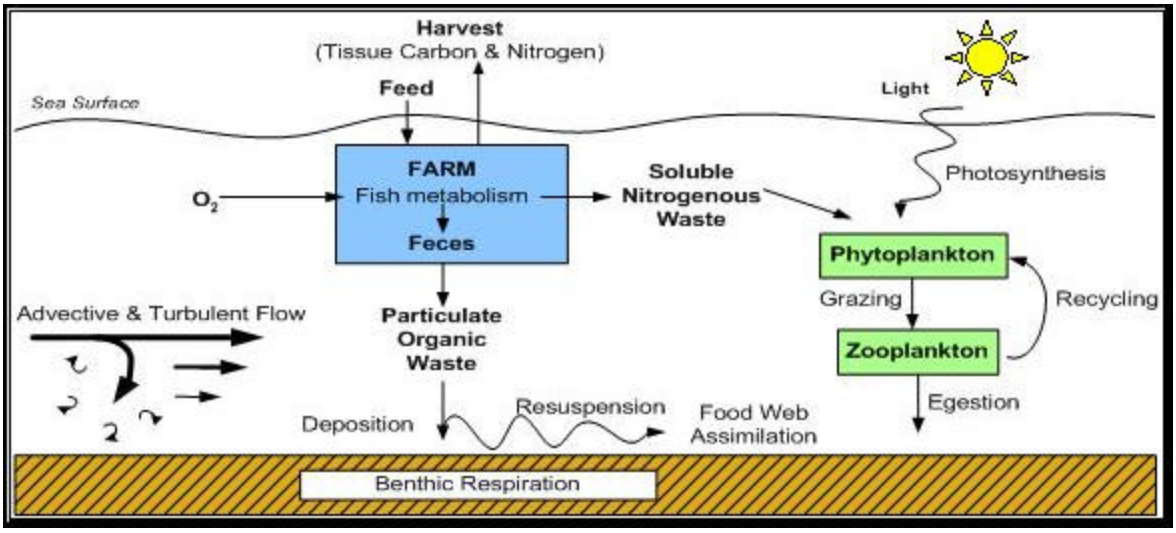

Figure 3. Components and transformations of water column and benthic submodels.

3.1 Fish Physiology Submodel

The component describing the growth and metabolism of the fish within the farm includes the processes of ingestion, egestion, assimilation, respiration, excretion, and growth (figure 4). Carbon, nitrogen, and oxygen fluxes are traced and interrelated, and rate functions vary with operational and environmental conditions. Operational conditions are the size and position of the farm, the daily rations, and the concentration and average size of the fish. Environmental factors that determine metabolic rates are current speed, the temperature of the water, and the concentration of oxygen in the water. As water passes through the farm, a "waste water plume" and a "waste particle plume" are created downstream. The characteristics of this plume will depend upon the metabolic activities within the farm as well as the advective and turbulent flows that shape the plume.

Five variables, the temperature of the water, the concentration of oxygen in the water, current speed, the average wet weight of the fish, their density within the farm, and the daily food ration define the initial state of the farm. Outputs from the simulation include 3 dimensional maps of the two types of waste plumes (dissolved and particulate) created by egestion, excretion, and respiration by the farmed fish. Outputs also include the growth rate and standing stock of the fish, and the concentrations of nitrogenous nutrients, oxygen, and particulate waste (feces) within the farm. Many plots of vertical profiles or transects can be viewed simultaneously, and all data can be written to spreadsheet or database to allow statistical and other types of post-model processing.

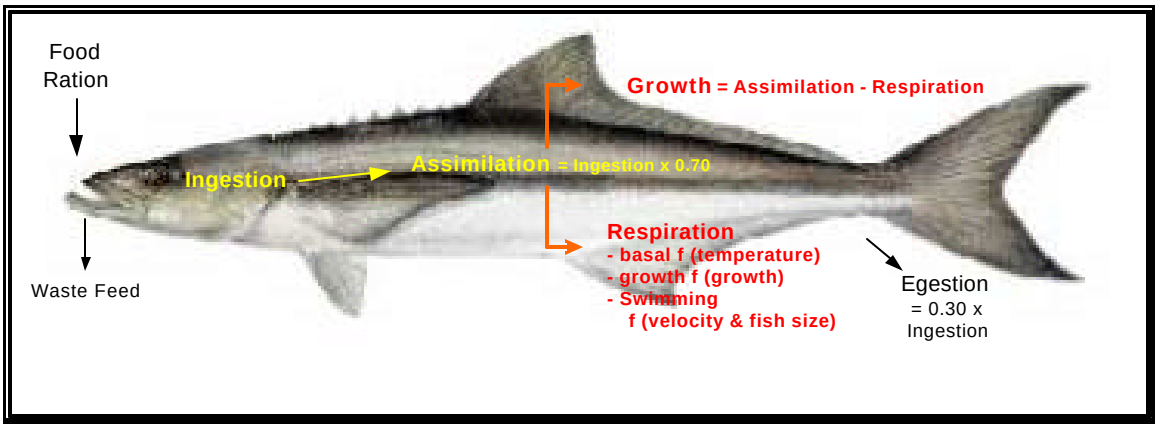

Figure 4. Generalized fish metabolic processes described by the model.

Growth rate information for cobia was obtained from several published or unpublished sources including FishBase (for von Bertalanffy (1938, 1960) growth rate characteristics and coefficients), Franks et al. (1999), D. Benetti unpublished Univ. of Miami PowerPoint on line, J. Forster, Forster Consulting pers. comm.). Over the first 9 months of life after seawater entry, the fish are capable of growing about 700 grams per month. This is a remarkably fast growth rate for any marine fish and we assume that the fish would be cultured at densities < 15 kg m^{-3} (~ 1 pound ft^{-3}) to be able to achieve such growth.

The cobia (*Rachycentron canadum)* AquaModel is a simulation of the metabolic activity of the fish grown within the farms. These metabolic activities include ingestion and assimilation of food, respiration, excretion and growth. These metabolic activities will vary with the operation of the farm. Operational factors are the size and position of the farms, the daily rations supplied to the stock, and the concentration and size of fish within the farm. Environmental factors that determine metabolic rates are current speed, the temperature of the water, and the concentration of oxygen in the water. As ambient water passes through the farm, a "waste water plume" will be created downstream of the farm. The characteristics of this plume will of course depend upon the metabolic activities within the farm as well as the advective and turbulent flows that shape the plume. The waste water plume describes the fate of two dissolved compounds, oxygen and nitrogen as nitrate, ammonia, or urea. The model also describes the fate of particulate waste including both fecal waste and uneaten feed. These particulate wastes sink as they are transported by the currents and will eventually be deposited to the sediments as particulate organic carbon and nitrogen. In the cobia AquaModel we have described this process in terms of particulate organic carbon, as carbon is the oxygen demanding component of the wastes. The metabolic processes of fish within the farm are described in terms of the transformations of carbon. Once these transformations are computed the associated transformations of oxygen and nitrogen are calculated by assuming a given stoichiometry for the ratio of elemental fluxes.

The initial state of the farms is defined by 7 variables:

- Water temperature, T
- Dissolved oxygen concentration, O_2,
- Advective velocity of the current,
- Turbulent advective velocity of the current,
- Average wet weight of the fish,

- Average density of fish within the farm, and
- Daily food ration delivered to the fish.

We chose to run simulations in which the temperature of ambient waters, the average concentration of fish, and the food ration were constant. Temporal variations in the concentration of O_2 within the farm are determined by the respiration of the fish, the flow of ambient water through the farm, and, to much lesser degree, planktonic rates of respiration and photosynthesis. Temporal variations in the wet weight of fish will of course be determined by their growth rate.

The metabolic processes that are mathematically formulated as a series of functions are well known in the field of physiological energetics. Specifically, the flow of carbon through the fish is described in terms of 5 metabolic processes that provide a budget for the transformations of carbon by the fish:

- ingestion rate = egestion rate + assimilation rate
- assimilation rate = rate of respiration + rate of growth
- respiration rate = resting rate of respiration (i.e. basal) + respiration rate of activity (i.e. swimming) + respiration rate of anabolic activity (i.e. growth)
- rate of feces production = egestion rate
- rate of loss of uneaten feed = feed rate – ingestion rate

We have chosen to represent each of these processes in terms of the specific rates of carbon flow, i.e. rate of carbon flux for a given metabolic process divided by the mass of organic carbon of the fish. We have also chosen to use units of gm-at C/(gm-at C*day), and since the units of mass are the same in the numerator and denominator, the units cancel out and are fluxes of per day units (1/day). We note that under steady state conditions the values for mass specific fluxes will be the same for other metabolized elements such as nitrogen and oxygen.

The rates of these processes are determined by the law of most limiting factor. Thus for example, the specific rate of ingestion is limited by either the size of the fish, the temperature of the water, the specific feed rate, or the concentration of oxygen in the water. Excess feed lost to current advection or overfeeding is added to the modeling process by setting the feed rate higher than the fish are able to ingest.

Table 1 contains the physiological key functions that describe the metabolic processes found in the equations above. Constants are shown in blue and input variables or arguments of each function are enclosed on the left hand side by square brackets. In order to focus attention on the key features of the functions, conversions factors for units (such as centimeters to meters) are not shown.

Table 1. Fish physiology submodel constants (in blue), input variables and equations.

(* Inputs *)

Efficiency of assimilation = 0.75 (dimensionless)

Reference weight = 500 g

aAssimilation = 0.04 / day

bAssimilationW = -0.4 / day

bAssimilation = 0.35 / C

Reference Temperature = 15 C

Transport coefficient = 1.4 cm / day

Gill oxygen concentration = 2 mg / l

bGillAreaW = -0.23 (dimensionless)

Kbucalflow = 10 cm / s

minimum bucal pumping rate = 25 cm / s

aBasal = 0.000164 / day

bBasalW = -0.4 (dimensionless)

bBasalT = 0.084 / C;

$$\text{aSwimmingspeed} = \frac{24\ \text{mg O2}}{\text{kgwet} * \text{day}}$$

bSwimmingspeed = 1.8 (dimensionless)

$$\text{Anabolic Demand} = 0.8\ \frac{\text{g C respired}}{\text{g C added}}$$

$$\frac{\Delta O2}{\Delta C} = \frac{1\ \text{M O2}}{\text{g-at C}}$$

$$\frac{\Delta N}{\Delta C} = \frac{1\ \text{g-at N}}{6\ \text{g-at C}}$$

$$\frac{\text{Carbon}}{\text{Weight}} = \frac{0.075\ \text{g C}}{\text{g wet weight}};$$

(* Independent Variables *)

Temperature of water

Ambient Oxygen concentration

Current velocity

Feed rate

Initial average weight of fish

Initial concentration of fish

Table 1 continued.

Carbon Supply

1. Assimilation rate [Weight, Temperature, Current speed, Oxygen concentration, Feed rate] = Efficiency of assimilation * Ingestion rate

2. Egestion rate [Weight, Temperature, Current speed, Oxygen concentration, Feed rate] = (1- Efficiency of assimilation) * Ingestion rate

3. Ingestion rate [Weight, Temperature, Current speed, Oxygen concentration, Feed rate] = the lesser of Feed rate or Assimilation rate, where the Assimilation is the lesser of functions 4 and 5.

4. Assimilation rate [Weight, Temperature] =

$$\left(aAssimilation * \left(\frac{Weight}{Reference\ Weight}\right)^{bAssimilationW}\right) /$$

(1+Exp [-b Assimilation * (Temperature- Reference Temperature)])

5. Assimilation rate [Weight, Current speed, Oxygen concentration] =

$$Transport\ coefficient * Gill\ Area\ per\ Weight * \left(\frac{Weight}{Reference\ Weight}\right)^{b\ GillArea\ W} *$$

(Oxygen concentration - Gill oxygen concentration)*

$$\frac{Buccal\ flow\ rate[Current\ speed, Weight]}{Kbuccalflow + bucal\ flow\ rate[Current\ speed, Weight]}$$

Respiration Demand

6. Resting Respiration rate [Weight, Temperature] =

$$aBasal * \left(\frac{Weight}{Reference\ Weight}\right)^{bBasalW} * e^{bBasalT * Temperature}$$

7. Active Respiration rate [Body length, Current speed] =

$$aSwimmingspeed * \left(\frac{Body\ length[Weight]}{Current\ speed}\right)^{bSwimmingspeed}$$

8. Anabolic Respiration [Weight, Temperature, Oxygen concentration, Current Speed] = Anabolic Demand * Growth Rate

Growth Rate

9. Specific growth rate [Weight, Temperature, Oxygen concentration, Current Speed]: = (Assimilation rate-Resting respiration rate-Active Respiration Rate) / (1+Anabolic Demand)

10. Food-limited growth rate [Weight, Temperature, Oxygen concentration, Current Speed] =

$$\frac{\text{Feed rate}}{\text{Optimal Feed rate}} * (\text{Assimilation rate} - \text{Resting respiration rate} - \text{Active Respiration Rate}) /$$

(1+Anabolic Demand)

11. Growth rate [Weight, Temperature, Oxygen concentration, Current Speed] =
Lesser of specific growth rate or Food-limited growth rate

Fluxes within the Farm

12. Rate of oxygen consumption [Weight, Temperature, Oxygen concentration, Current Speed, Fish concentration] =

$$\frac{\Delta O2}{\Delta C} * \text{Fish concentration} * \text{Weight} * \frac{\text{Carbon}}{\text{Weight}}$$

(Resting respiration rate + Active Respiration rate + Anabolic Demand * Growth rate);
(e.g. g O2/(m3*day))

12. Rate of dissolved nitrogen production [Weight, Temperature, Oxygen concentration, Current Speed, Fish concentration] =

$$\frac{\Delta N}{\Delta C} * \text{Fish concentration} * \text{Weight} * \frac{\text{Carbon}}{\text{Weight}} *$$

(Resting respiration rate + Active Respiration rate + Anabolic Demand * Growth rate); (e.g. g-at N / (m3*day))

14. Rate of Feces production [Weight, Temperature, Oxygen concentration, Current Speed, Fish concentration] =

Fish concentration* Weight* $\frac{\text{Carbon}}{\text{Weight}}$ * Egestion rate; (e.g. g C / (m3 * day))

The first 5 functions in Table 1 determine the specific rate of carbon assimilation by the fish. Functions 1 and 2 describe the rates of assimilation and the rates of egestion. Both are functions of the rate of ingestion and the efficiency of assimilation, a constant equal to 0.75. As indicated in function 3, the ingestion rate is itself a function of all the independent variables, temperature, oxygen concentration within the farm, current speed, the average weight of fish within the farm, and the feeding rate. Specifically, it is the lesser value for the feeding rate or the rate of assimilation, and in turn the rate of assimilation is the lesser value for the rate of assimilation as determined by the weight and temperature of the water or as determined by the transport of oxygen.

Function 4 describes the specific assimilation rate as determined by the weight of the fish and the temperature of the water. The numerator on the right hand side of the function describes the dependence upon the weight of the fish; it is a power function. The denominator describes the

dependence upon the temperature of the water. Fish of a given size in cold water assimilate carbon more slowly than those are warmer temperatures. The shape of the temperature response is sigmoidal curve that is characterized by its slope and a reference temperature.

Function 5 describes the specific assimilate rate as determined by the rate of transport of oxygen across the gills. The first 4 terms on the right hand side of the function describes the dependence of oxygen transport on the surface area of gill per unit weight for fish of a given weight and the concentration gradient between the aqueous concentration of oxygen and the gill's lamellae. This dependence is essentially Fick's Law of Diffusion in which the rate of diffusion is the product of the diffusion coefficient, surface area, and concentration gradient. The final term on the RHS addresses the surface boundary layer that occurs between the gill's surfaces the water that is passing through the gills. If water flows or is pumped rapidly through the buccal cavity the boundary layer will be reduced and the transport of oxygen will be faster. We have described this dependence as a hyperbolic tangent in which rates increase linearly with flow at low pumping rates and saturate at high pumping rates. As indicated flow rate of water through the buccal cavity will be a function of the swimming speed and the weight of the fish. Below a threshold value of swimming speed buccal pumping will determine the flow rate through the cavity. The respiratory cost of buccal pumping is included in the resting respiration rate (Equation No. 6).

The next 3 functions describe the rate of respiration. Function 6 is the resting respiration rate; it is determined weight and temperature in which respiration is scaled to the weight of the fish by a power law and scaled to temperature by an exponential law. Both laws are common in physiological literature. We assume that this basal rate of respiration includes the cost of buccal pumping but not the cost of anabolic respiration.

Function 7 describes the respiration required by swimming. This power law was taken from the publications of Gill and collaborators; the rate is determined by the length of the fish, a function of weight and not shown in table, and the current speed. We have assumed that the fish in the farm maintain their position within the farm and thus must swim at the rate of current speed. Function 8 describes the respiration required by growth; it is simply the product of a constant, the anabolic demand (equal to 0.8 g-at of carbon for each g-at. of additional carbon biomass) and the growth rate.

The next 3 functions determine the growth rate. Function 9 describes the natural growth rate, defined as the growth that would occur if the fish were provided food at a rate equal to (the "optimal feed rate") or greater than the rate necessary to achieve maximal growth rates under ambient conditions. As indicated this function is simply the difference between the assimilation rate and the sum of the respirations rates for resting, active, and anabolic metabolism. Function 10 describes the food-limited growth rate- simply the product of the ratio of the feed rate to optimal feed rate and the natural growth rate. Logically as shown in function 11, the growth rate of the fish is the lesser of these two rates.

The final 3 functions describe fluxes (units of mass/(m^3*day) within the farm that are coupled to the specific rates of carbon transformations. The fluxes of oxygen consumption, nitrogen excretion, and fecal carbon production are simply the product of stoichiometry ratio of the flow of the element or compound of interest to the associated flow of carbon (e.g. oxygen consumed to carbon released as carbon dioxide), the specific rate of carbon flow, and the concentration of fish carbon within the farm.

3.2 Outputs from the Cobia Physiology Submodel

We outline in the figures below the behavior of the Cobia model. Figure 5 is the von Bertalanffy growth curve for *Rachycentron* from birth to 7 years of age. The parameters for the function were obtained from FishBase, but tuned for information on the rapid growth that occurs in farms. It is indeed a fast growing fish. See the FishBase website at: http://www.fishbase.org/Summary/speciesSummary.php?ID=3542&genusname=Rachycentron&speciesname=canadum,

Figure 6 is second representation of growth rate in which the specific growth rate is plotted against the weight of the fish at its respective age. Two curves are plotted; one is output of the cobia model, and the other is derived from the von Bertalanffy growth curve shown in figure 5. In spite of the complexity of our cobia model, the agreement is obviously very good. Figure 7 is a plot of the calculated specific growth of a 500 g. cobia growing at 28 C as determined by variations in specific feeding rate. A maximum growth rate of about 2 % /d saturates at a feeding rate of about 4.5 % day. There are numerous other outputs of Cobia AquaModel, that include predictions of such features as growth rate and rates of respiration, and excretion as determined by temperature, oxygen concentration, and current speed. These outputs are of key importance not only to assess the ecological impact of the farm, but also to determine successful operations of the farm.

Unfortunately, the database on cobia physiology and growth is small and insufficient to provide a rigorous test of the model. On the other hand, data on Atlantic salmon physiology and growth is extension and our model proved remarkably accurate in fitting observations.

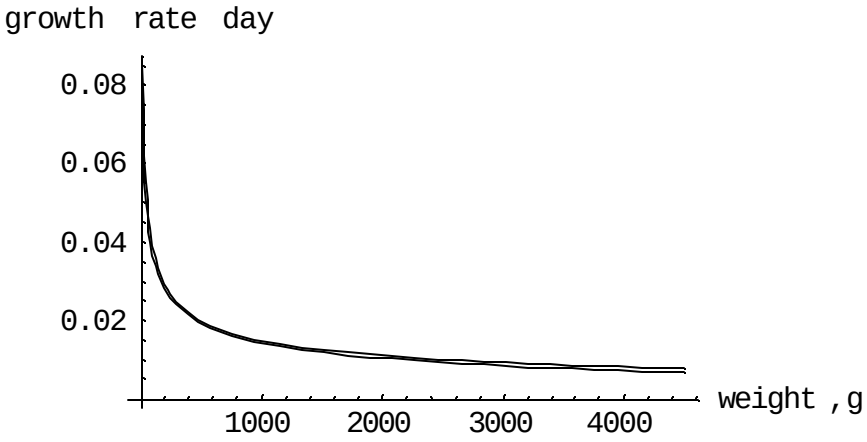

Figure 5. The von Bertalanffy growth curve for cobia tuned to fit selected data from growth in fish farms.

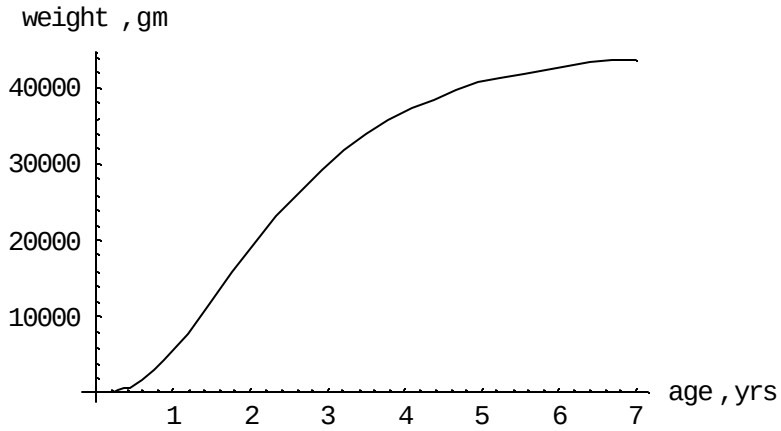

Figure 6. The specific growth rate of cobia as a function of weight at age.

Two curves are plotted, one is calculated from our cobia model the other is derived directly from the von Bertalanffy growth curve shown in the figure above.

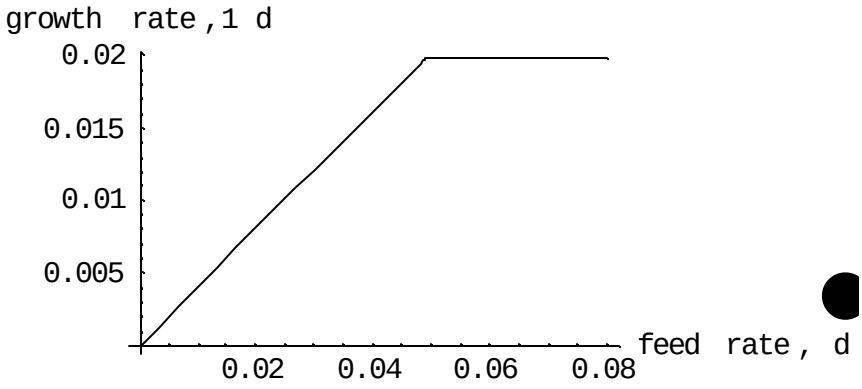

Figure 7. The calculated specific growth rate of cobia as a function of specific feed rate.

Temp. 28°C, weigh 500g, good growth efficiency exhibited.

3.2. Plankton Module

The plankton module (Fig. 3) describes the cycling by plankton of nitrogen and oxygen within each element of the array, both within the farm and the surrounding waters. This model is similar

to the PZN models that have been published by Kiefer and Atkinson (1984) and Wroblewski, Sarmiento, and Flierl (1988). The "master" cycle describes the transforms of nitrogen between three compartments, inorganic nitrogen, organic nitrogen in phytoplankton, and organic nitrogen in zooplankton. The three biological transforms are:

- Photosynthetic assimilation of inorganic nitrogen by phytoplankton which is a function of temperature, light level, DIN (dissolved inorganic nitrogen consisting of ammonia, nitrite and nitrate) concentration
- Grazing by zooplankton on phytoplankton which is a function of temperature and concentrations of zooplankton, and phytoplankton
- Excretion of DIN by zooplankton, which is a function of temperature and the concentration of zooplankton.

All three compartments are transported by advective and turbulent flow as described above. The model displays predator-prey oscillations, which dampen over time and reach a steady state. The default simulations for DIN, phytoplankton, and zooplankton stabilize at roughly 0.1 mg-at N-at m^{-3}, 0.1 mg-at N m^{-3}, and 0.1 mg-at N m^{-3}, respectively. In order to calculate the concentrations and rates of loss by respiration and production by photosynthesis, we have assumed a constant flux ratio of oxygen to nitrogen of 6 moles O_2/gm-at N, consistent with the Redfield ratio. As indicated in the accompanying table, the inputs to this model consist of the time series of exchange coefficients produced by the hydrodynamic model, surface irradiance, and water temperature as well as concentrations of dissolved oxygen, dissolved inorganic nitrogen, cellular nitrogen in phytoplankton and zooplankton. Outputs of this model consist of a time series of the concentrations of dissolved inorganic nitrogen and oxygen, phytoplankton (traced as chlorophyll), and zooplankton. Since plankton dynamics proved to play a very small role in the present simulation, we have chosen not to describe the system of equations in any detail.

3.3 Hydrodynamic Submodel

Model simulations occur within a 3 dimensional array of rectangular elements, the grid) whose dimensions and location are also user-defined. The time steps for the simulation vary between 1 and 5 minutes depending upon the speed of the currents. The array we used to examine the OHA cobia fish farm was 3,253 m. in length, 2,676 m. in width, and 30 m. in depth, which is the depth of our simulated water column. This array contains 9,486 elements that were 104 m in length, 52 m in width and 5 m in depth. The center element of the array at +18.055 latitude and –65.771 longitude contains the 10 farms. The simulated pens will be centered at depths of 5 m. below the surface at their most shallow depth and 15 m. below the surface at their deepest depth. The advective and turbulent flow in the region carries water and dissolved and suspended particles between elements of the array. In addition, water and materials are accordingly moved across the side boundaries of the array; however, here the values for the concentrations of dissolved and particulate materials at the boundaries remain constant and equal to the values that are entered by the user at the start of the simulation. Thus, within the elements of the array that are not located at the boundary, the condition of conservation of mass for dissolved and particulate material is maintained. On the other hand, this condition is not maintained at the boundary. This is a constraint of most if not all circulation models.

The bottom boundary of the array is treated differently since this is the interface between the processes that occur within the overlying water column and the processes that occur within the sediments. Specifically, this is the boundary where transport, deposition and resuspension of particulate waste from the farm occur. This bottom boundary layer has complex dynamics that are crudely formulated in the Cobia AquaModel. As discussed in section 3.4, the benthic submodel, contains functions describing the processes both within the surface layer of the sediment and the overlying aqueous boundary layer.

The system of equations describing circulation is a simple finite element description of advection and dispersion. Each element of the array is treated as a box model in which materials flow across the 6 interfaces of each element, top, bottom and the four sides. Each element is treated as instantly mixed throughout. The basic equation describing the change in concentration with time is based upon the "transport equation', shown below in Table 2.

Table 2 . Hydrodynamic model components and equations.

$$\frac{\Delta C_i}{\Delta t} = \frac{1}{Volume_i} \sum_{j=1}^{j=6} Area_{ij} \left(v_{j \to i} C_j - v_{i \to j} C_i\right) + S_i + Area_{top}\, v_{sinking} \left(C_{top} - C_i\right)$$

C_i is the concentration of tracer material within element i

C_j is the concentration of dissolved or particulate material within adjacent element found at each of the 6 sides

$Volume_i$ is the volume of element i

$Area_{ij}$ is the area of the interface between elements i and j

$v_{j \to i}$ is the velocity of water both advective and turbulent that passes from j to i

$v_{i \to j}$ is the velocity of water both advective and turbulent that passes from j to i

S_i is the rate of production (or consumption) of the tracer within element i

$Area_{top}$ is the area of the interface between element i and the element above it

$v_{sinking}$ is the sinking velocity of the particle

C_{top} is the particle concentration in the element above element i

The first term on the right hand side of the equation is the change in concentration of the tracer (e.g. inorganic nitrogen, oxygen, fecal particle) during a time step caused by turbulent and advective exchange across the 6 sides of the element. The second term is the change cause by local consumption or production of the tracer, and the third term is the change caused by sinking of a particle tracer.

Advective flow is described as a net movement of water in which the inflow and outflow of water differs among the 6 sides of the element; in other words v(i->j) is not equal to v(j->i). Turbulent flow on the other hand is described by the condition where there is no net movement of water across the interface; in other words in other words v(i ->j) is equal to v(j->I).

Advective flow in many coastal and near offshore areas is largely determined by tides or by wind-driven currents. The direction of flow likely change with time, and in the case of tidal flow these

changes can be accurate predicted. As described below inputs to the model of the time series for advective flow were obtained from field measurements of the track of a drogue at the OHA site. Advective velocities vary between 0 to more than 50 cm s^{-1} as described later in this report.

We have assumed that turbulent flow is isotropic in the horizontal; thus the exchange coefficients of the 4 vertical sides of element were equal. On the other hand vertical dispersion varied depending upon whether the element is within the surface mixed layer or within the underlying water column. In addition, the vertical exchange coefficients at the surface and the bottom of the water column are zero. We have also assumed that the velocity of turbulent exchange between adjacent elements of the array increases with increasing advective velocity; in other words, the turbulent component of vi->j is a specified fraction of the advective velocity. We argue that this scaling of turbulence is valid in coastal waters where increases in flow cause increases in bottom drag that will likely spin off larger and more eddies. This fraction is selected by the user for turbulence in the horizontal direction, as well as the vertical direction with both the mixed layer and the stratified deeper waters.

We have used the data on the rate of separation of multiple drogues deployed at the same location to estimate turbulent exchange velocity in the horizontal direction. In addition, ADCP data (vertical current meter profiles) and water temperature casts at the OHA site suggests that the water column is well mixed to close to the bottom, and thus, we have set the depth of the surface mixed layer is 30 m. In the simulations of the Cobia AquaModel the turbulent exchange velocity in the horizontal is 0.1 that of the horizontal advective velocity, and the turbulent exchange velocity in the vertical (mixed layer) is 0.05 that of the horizontal advective velocity.

3.4 Benthic Submodel

The benthic loading component of our model is based upon several literature citations and functions found in the existing, well-verified DEPOMOD model (Cromey et al. 2002a, 2002b) that in turn was based on the G-model of carbon degradation (Westrich and Bernier 1984 and subsequent papers). Despite some limitations involving lack of user control and flexibility, DEPOMOD is presently the international standard for assessing the impact of loading of organic carbon in sediments underlying fish farms and is required by some foreign jurisdictions prior to permit issuance. Since the DEPOMOD model is proprietary and does not include any water column effects simulation, we have written our own code to describe the benthic-particulate matter-carbon distribution and degradation processes. This code consists of functions describing:

- Production of particulate wastes within the farm.
- Movement of these wastes away from the farm by the process of sinking and transport via ambient advective and turbulent flow.
- Deposition of these wastes to the sediments within the benthic boundary layer.
- Biogenic respiratory loss of particulate organic wastes within the water column and within the sediments.
- Resuspension of wastes that have been deposited in the sediments by ambient advective flow by stronger tides or ocean currents.
- Transport of the resuspended wastes via ambient advective and turbulent flow and repetition of the sedimentation, erosion and carbon degradation cycle.

We have not included consolidation (i.e., compaction/accretion) of waste because little is known about this process and because the OHA site is characterized by relatively strong currents that cause periodic resuspension of solids. Such sites have coarse sand or gravel/rock seabottoms, and the OHA site is reportedly coarse sand. As discussed later in this report, current meter and acoustic Doppler current meter results from the OHA site are relatively strong throughout the water column including near the sea bottom. A consolidation factor would be required in depositional sites such as those in some Norwegian, Scottish or British Columbia sea lochs and was used by Riedel and Bridger (2003), but is not needed in more active sites such as the subject site in Puerto Rico.

The production of particulate wastes by the farm consists of uneaten feed and egestion, and the rate of waste production is an output of the fish metabolism component described above. According to the fish metabolism component, ingestion rates will be a function of not only the size and concentration of the fish, but also their capacity to assimilate food as determined by water temperature, swimming speed, and the supply of dissolved oxygen. If the capacity of the fish to assimilate food is greater than the feed rate, the growth rate of the fish is "food-limited", and there will be no wasted food. If the feed rate exceeds ingestion rate, the excess food will contribute to particulate wastes. The rate of egestion (defecation) is simply a fixed fraction of ingestion based on expected values from the literature.

Values for the sinking rate of feces and food pellets are determined from measurements both in the laboratory and field. The sinking rates of feces varies greatly with species or major taxa of fish; for example the mean sinking rates of salmonid species is at least three to six times greater than rates of many marine fish (Magill et al. in press, Rensel unpublished sablefish data, D. Benetti pers. comm.). As the feed and fecal wastes sink through the water column, ambient currents and turbulent motion will disperse them horizontally and vertically forming a plume down stream. Flow velocities, the depth of the water column, and sinking velocity will largely determine the initial distribution of waste that reaches the bottom.

Deposition of waste to the sediments occurs within the bottom boundary layer, and the rate of deposition is a function of the shear at the sediment-water interface. If the shear falls below an experimentally determined threshold value for a certain size and density of particle, deposition will occur. Below this threshold, the rate of deposition increases with decreases in shear and increases in the concentration of particles within the boundary layer. Bottom shear itself is proportional to the square of flow velocity at the interface, and the flow velocity at the bottom is estimated from the flow velocity at a reference depth above the bottom. Resuspended wastes will be transport away from the site of deposition by ambient flow until flow rates once again fall below the threshold for deposition. If, as is the case of our simulation of a feces deposition beneath a salmon farm, the threshold for resuspension is considerably larger than the threshold for deposition, there exists bed shear velocities at which neither deposition nor resuspension will occur. Under such conditions waste remains in suspension near the bottom, and are transported away from the farm while being oxidized by bacteria and assimilated by the benthic/demersal food web. Since in many cases the flow at farms is dominated by tides, water current velocities will vary with the tide, and periods of deposition and resuspension may alternate accordingly.

Respiration of waste carbon is mediated by plankton in the water column and by the benthos, in the sediments. The rate of respiration both within the water column and the sediment is described according to the G-Model of Westrich and Bernier (1984) and subsequent papers. According to

this model, the rate of respiration will depend upon composition of the particulate organic material: labile compounds will be respired at rates faster than refractive compounds. Each class of compound, labile or refractive, will be respired according to a first order reaction in which the rate of loss is a function of the product of the concentration of the compound and its rate constant. Thus the loss of particulate wastes by respiration is described as the sum of the respiration rates for each of the compounds. Fish feces carbon is relatively labile (Tlusty et al. 2002) and most of it is rapidly respired by the benthos.

The amount of waste carbon that accumulates in the sediments in the vicinity of the farm is described as the interaction between the processes outlined above.

$$\frac{\Delta Cwaste}{\Delta t} = deposition - re\min eralizatio n - resuspension$$

This formula says the change in the carbon waste concentration in the sea bottom over time is equal to the deposition rate, which is a function of the velocity of water flow, rate of waste production, settling rate, and the rate of respiration loss within the water column, minus the benthic respiration of carbon wastes, which is a function of the concentration of waste in the sediment, minus resuspension, which is a function of the concentration of waste in the sediment and benthic shear velocity.

As implied by the arguments in the right hand side of the above equation, respiration rate and resuspension increase with increases in the amount of waste carbon in the sediment. Thus, there exists a value for the amount of waste in the sediment when deposition rates are equal to the rates of loss by resuspension and respiration. At that point a steady state condition is established, thereby determining an upper limit to waste accumulation in the sediments for given environmental and operational conditions.

The key equations are shown in the Table 3 below. There are two principal types of particle waste produced by the farms, uneaten feed and feces. The fate of these wastes are determined by 5 major processes that determine produced by the farms: the rate of particulate waste production by the farms, the sinking speed of the particles, the advective and turbulent transport of particles from the farm, the conditions for deposition and erosion within the bottom boundary layer, and the rate of remineralization of suspended and deposited particles. As was the case for the Cobia growth model, constants are shown in blue.

Function 1 describes the relationship between the *Bottom shear speed*, which determines whether the transport of particles at the bottom will remain in suspension, be deposited, or be augmented by resuspension of the particles that have previously been deposited. Since the current speed at the bottom is not easily measured this speed is estimated by measuring current velocity, the *Measured shear speed*, that is measured at referenced distance above the bottom, *Distance above bottom*. The *Measured sheer speed* is then extrapolated as a logarithmic decay to the value at the bottom water interface. The shape of the Logarithm function is determined by the ratio of the *Distance above bottom* to the *Bottom roughness* diameter, and the value of the *Bottom shear* speed is scaled by the *von Karman constant*. Function 2 describes the *Bottom shear*, the critical parameter of particle deposition and erosion, as simply the product of the density of seawater and the *Bottom shear velocity.*

Table 3. Benthic submodel constants and equations

(*Inputs*)

Distance above bottom = 200 cm

water density = 1025 (*kg/m3*) ;

von Karman constant κ = 0.4 (dimensionless)

Deposition shear velocity threshold = 3 cm / s

Erosion shear velocity threshold = 6 cm / s

hydrodynamic roughness = 0.0002 cm (Soulsby 1983)

Maximum Particle erosion rate = 0.0050 kg - atC / (m2 * day)

Particle sinking speed = 1 cm / s

Deposited particles remineralization rate = 0.01 / day

Suspended particles remineralization rate = 0.01 / day

(*Functions*)

1. Bottom shear speed[Measured shear velocity] =

$$\frac{\text{von Karman constant} * \text{Measured shear velocity[Distance above bottom]}}{\text{Log[Distance above bottom / Bottom roughness]}}$$

2. Bottom shear[Bottom shear velocity] = water density * Bottom shear velocity^2

3. a. If Bottom shear > Deposition shear threshold, then Deposition rate = 0

3. b. If Bottom shear <= Deposition shear threshold, then

Deposition rate[Suspended particle concentration, Bottom shear, Particle sinking velocity] =

$$\frac{\text{Suspended particle concentration} * \text{Particle sinking velocity} * (1 - \text{Bottom shear})}{\text{Deposition shear threshold}}$$

4. a. If Bottom shear velocity > Erosion shear threshold,

and If $\frac{\text{Maximum erosion rate} * \text{Bottom shear}}{\text{Erosion shear threshold} - 1} <$ Accumulated particle mass,

then Erosion rate[Bottom shear] =

$$\frac{\text{Maximum erosion rate} * \text{Bottom shear}}{\text{Erosion shear threshold} - 1}$$

4. b. If Bottom shear velocity > Erosion shear threshold,

and If $\frac{\text{Maximum erosion rate} * \text{Bottom shear}}{\text{Erosion shear threshold} - 1} \geq$ Accumulated particle mass,

then Erosion rate[Deposited particle mass] = Deposited particle mass

4. c. If Bottom shear <= Erosion shear threshold, then Erosion rate = 0

5. Deposited particle remineralization rate[Deposited particle mass] =

Remineralization rate constant * Deposited particle mass

6. Suspended particle remineralizatin rate[Suspended particle concentration] =

Remineralization rate constant * Suspended particle concentration

Function 3.a. and 3.b. are a conditional description of particle deposition. If *Bottom shear* is greater than a threshold value that is characteristic of the particles, *Deposition shear threshold*, then the particles will remain in suspension (3.a.), and if the shear is less than this threshold the particles will be deposited at a rate that is proportional to the product of the concentration of particles immediately above the bottom, *Suspended particle concentration*, the sinking velocity of the particles, *Particle sinking velocity*, and 1- *Bottom shear*.

Function 4.a., 4.b., and 4.c. are a nested conditional description of entrainments of particles that have been previously deposited in the sediment into the overlying water, *Particle erosion rate.* 4.a. and 4.b. state that if *Bottom shear* exceeds the *Erosion threshold shear*, then particles will be entrained and thus transported from the most recent site of deposition. 4.c. states that if *Bottom shear* is equal to or less than the *Erosion threshold shear*, then particles will not be entrained. The difference between 4.a. and 4.b. concerns the rate of entrainment of particles. This distinction is based largely upon mass of particles on the bottom, *Accumulated particle mass*. If as in 4.a. the *Accumulated particle mass* exceeds the amount that would be entrained during the time interval that entrainment occurs, then the *Particle erosion rate* is simply the product of a constant, *the Maximum erosion rate*, and *Bottom shear*, divided by 1-*Erosion shear threshold*. On the other hand, if as in 4.b. the *Accumulated particle mass* is less that the amount that would be entrained during the time interval that entrainment occurs, and then the *Particle erosion rate* is equal to the *Accumulated particle mass.* In other words all deposited particles are resuspended.

The combined processes of erosion and deposition clear define 3 conditions at the sediment interface as follows:

- At the lowest current speeds deposition occurs and rates of deposition vary inversely (not linearly however).
- At intermediate current speeds neither deposition nor erosion occurs. Particles remain in suspension and are transported away from their current location,
- At higher current speeds deposited particles are resuspended or entrained into the overlying water and are transported rapidly away from the site of previous deposition.

Our measurements and calculations indicate that all 3 conditions will occur at the OHAI site.

Function 5 describes the rate of remineralization of particles that have been deposited into the sediment. The rate is a simple first order rate of reaction, the product of a *Remineralization rate constant* and the *Deposited particle mass*, i.e. mass of particles in the sediment. Remineralization is the respiration of organic material by microscopic living in the sediments as well as macroscopic organisms feeding off the bottom or within the sediments. This loss term insures that there is exists an upper limit to the mass of particles in the sediment. This mass is determined by the condition steady state at which the rate of remineralization is equal to the rate of deposition.

Function 6 describes the rate of remineralization of particles suspended in the water column. The rate is a simple first order rate of reaction, the product of a *Remineralization rate constant* and the *Suspended particle concentration*. This remineralization is the combined respiration of organic material found in both fecal and uneaten feed, by microscopic and macroscopic plankton and nekton. The value for the rate constant for uneaten feed is likely to be much higher than the value

here, because it is well know that natural stocks of fish often aggregate at farms and consume feed that escapes the farm.

4. Prior Model Calibration

We define model calibration as the process of incorporating the appropriate local conditions (i.e., the ambient current velocity, water temperature, dissolved oxygen, depth, depth of mixed layer, diffusion gradients, etc) as well as farm site description (i.e., area and volume of farm, depth of nets, orientation of the array of cages, etc). For our model it also includes using the most appropriate fish physiology components such as the interaction of temperature, ration, fish size, respiration rate and waste production rates.
The intent of the model calibration process is to refine the model "to achieve a desired degree of correspondence between the model output and actual observations of the environmental system that the model is intended to represent" (EPA 2002). In the process of gathering calibration factors or data, we used local Puerto Rico experts and others engaged in current research and monitoring. These data are summarized below but here we provide some introductory and background information to supplement the tabular information.

Model calibration is a dynamic process and we seek the best available data for every application each time the model is modified. As there is scant literature on water and sediment quality for the subject area, we consulted with Dr. Jorge Capella regarding hydrographic conditions in the area and also used his current meter records for the proposed project site. He provided published and unpublished data cited below and general advice on conditions at the site such as the dominance and importance of M2 tidal energy in controlling water motion. We collected acoustic Doppler current meter data throughout the modeling domain too. We found that current velocity at mid water column (where Dr. Capella's current meter was located) is similar to near bottom velocity (J. Rensel unpublished ADCP data from 18 and 19 October, 2005). Water temperature, ambient dissolved inorganic nitrogen, phytoplankton biomass (as measured by chlorophyll *a* pigment concentration), mixed layer depth in the subject depths in Puerto Rico vary little over the calendar year. This allows us to neglect some seasonal changes that we have used in temperate water applications of the model. Depth at the subject site is relatively constant too, allowing us to assume a constant bathymetric profile in the modeling domain.

For cobia physiology, we reviewed all available literature and contacted several experts regarding growth characteristics. Although recent respiration and excretion studies have been completed on small juvenile cobia (<20 g), no data was available for larger juveniles or subadults. Accordingly, we revised our existing salmonid model to account for the higher temperatures to be encountered in Puerto Rico (28°C versus 13 to 15°C), which resulted in somewhat greater than a Q_{10} doubling of metabolism and waste production commensurate with the much faster growth. The uncertainty regarding waste production of older cobia is offset in our model by using higher than mean biomass values that would be encountered later in the production cycle. Our model is based on solid physiological underpinnings, i.e., that there is only a set amount of carbon input in the feed for bioenergetic mass balance, which is distributed among growth, basal metabolism, swimming and other energy demanding activities (Alexander 1967). This is discussed in more detail above in the fish physiology submodels sections 3.1 and 3.2.

5. Prior Model Validation

As in any simulation model, testing and validation is necessary (Chromey and Black 2005, Rensel et al. in press b). Testing and validation of our model has been done in several stages. First, it is conducted upon initial equation development when we create mathematical formula to characterize known physical and biological processes

As noted above, our model was initially designed for use with salmonids in temperate waters. This choice was made in part because there is a rich literature of physiology and impact studies to draw upon in constructing the fish physiology, water quality and benthic submodels. The physiology of cobia is not as well known or described as that of the Pacific and Atlantic salmon, but growth and feed conversion are known to some degree of certainty for the first year of life. We present the following to demonstrate that the model has been validated in other circumstances.

The series of equations describing growth and metabolism were written by us and based upon published field and laboratory data on the rates of growth, feeding, and respiration of salmonids under differing conditions of temperature, feed rate, oxygen concentration, and swimming speed. These include repeated measurements of oxygen and nitrogen plumes collected by one of us (JER) over several years at several different commercial fish farms while concurrently measuring current velocity and linearity of flow (i.e., to insure laminar flow from up to downstream). Most of these functions found in our system of equations are well known while a few "missing relationships" were derived by applying general physiological principles. Having been involved in over two decades of water column and benthic effects studies, many at the same farms, we were able to inspect model outputs over a range of loading and operating conditions to estimate model validity. We have also conducted measurements of horizontal dispersion of water masses downstream of fish farms to calibrate the model waters near surface cages. Our few estimates are similar to those recently published by Cromey and Black (in press) who found dispersion coefficients in tropical waters varied from less than 0.01 $m^2 s^{-1}$ to greater than 0.4 $m^2 s^{-1}$ for the most dispersive site studied in the Mediterranean Sea. Other measurements in Scottish fjiordic sea lochs that are dominated by macrotidal conditions resulted in measurements between 0.1 and 0.7 $m^2 s^{-1}$. The most dispersive MERAMED site falls within the middle of this range.

Our comparison of predictions of growth and metabolic activity for fish (salmonids) growing over a broad range of environmental conditions with published data displayed good agreement (Rensel, et. al. in Press a). Figures 8 and 9 show two comparisons of model predictions with laboratory measurements. Figure 8 shows predicted (dashed lines) and measured (solid lines) growth rates for young sockeye salmon grown at different temperatures (abscissa) and different feed rates (legend). The growth rates are in units of the fractional change in body weight per day, and the feed rates of 0.06, 0.03 and 0.015 are in units of fractional body weights of food per day. Note that the model accurately predicts the decreases in the temperature of optimal growth with decreases in feed temperature. The predicted growth rates are calculated from the functions describing all the physiological aspects shown in figure 8.

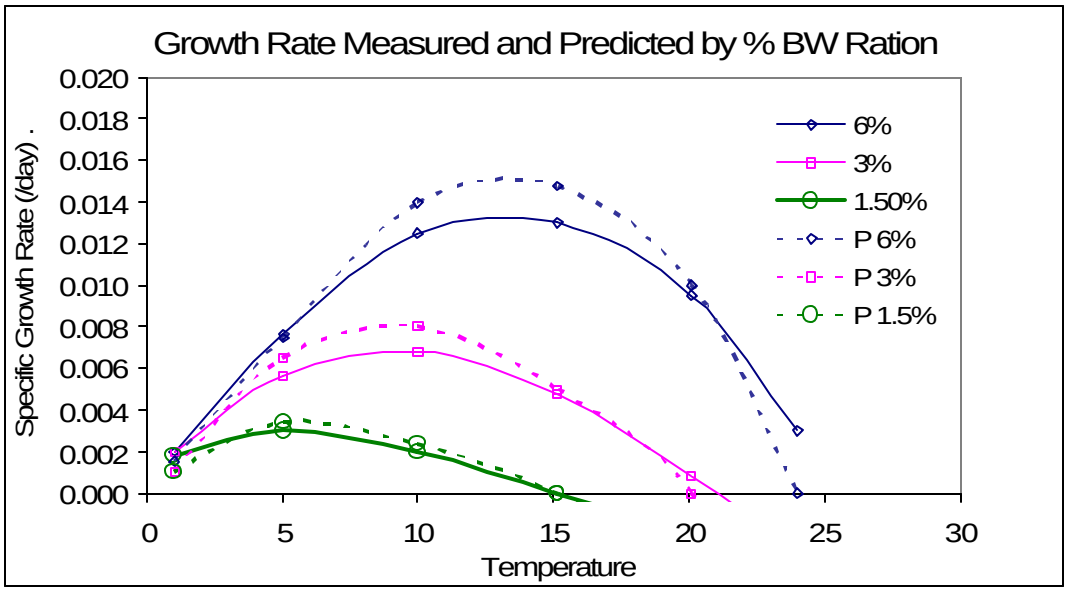

Figure 8. Growth rate measured in culture versus predicted (P) by model for initial calibration runs.

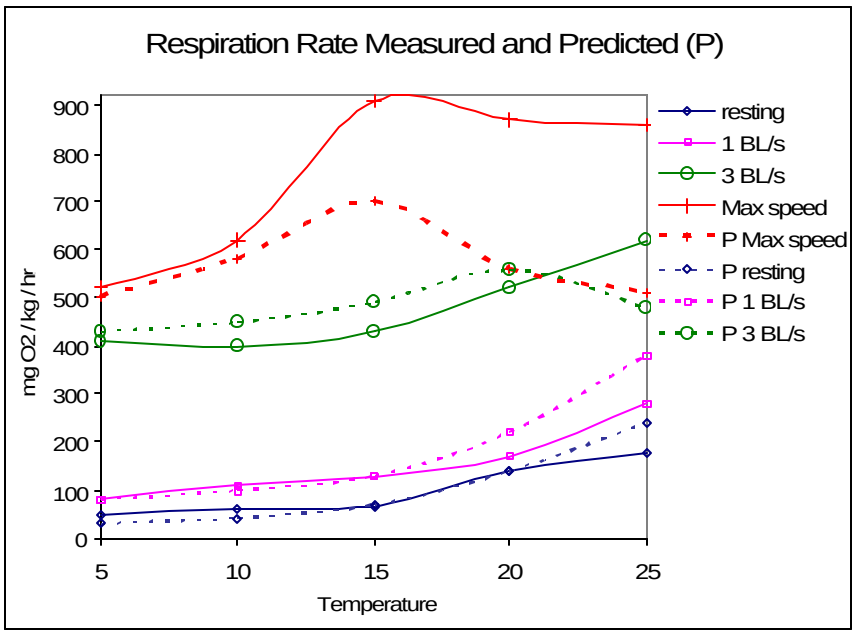

Figure 9. Laboratory measured vs. model predicted (P) respiration rate for initial calibration runs.

Figure 9 shows predicted (dashed lines) and measured (solid lines) respiration rates for young sockeye salmon swimming at different speeds (legend) and at different temperatures (abscissa). The swimming speeds found in the legend are in units of body lengths per second. The upper graph shows respiration rates for maximum swimming speed record for a given temperature.

Although our model describes steady state conditions as opposed to the short time interval during which the measurements was made, the fit is still good except at maximal swimming speeds. This was modified for Puerto Rico and the subject fish species (cobia).

Rensel (in WDF 1991 appendices and subsequently collected unpublished but reported NPDES monitoring data) has examined nutrient and dissolved oxygen deficit plumes around commercial net pen farms. In both cases the extent to which the plume can be detected is typically less than 30m for these large farms with 1,000 MT (2.2 million pounds) or more of fish biomass as shown in Figures 10 and 11, respectively. For dissolved oxygen, thousands of measurements have been collected in Maine by C. Heinig, yielding similar results (Normandeau Associates and Battelle 2003).

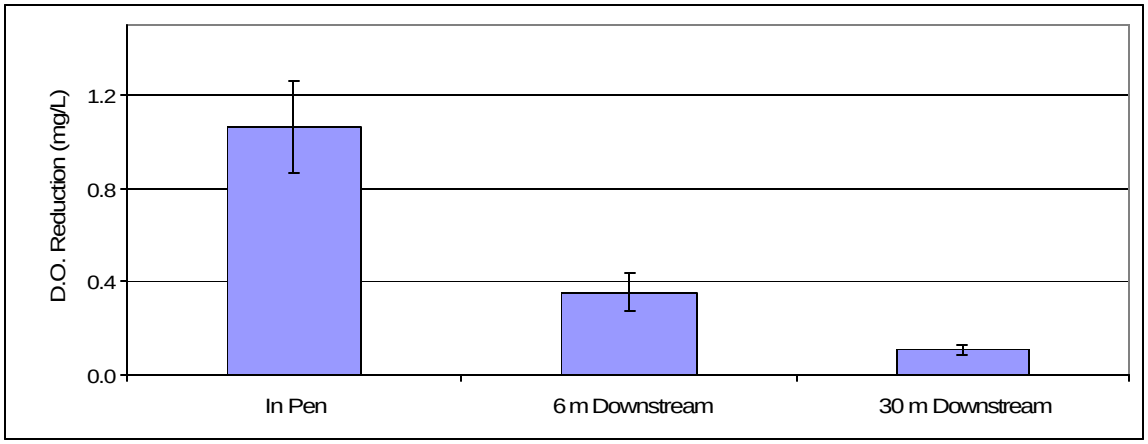

Figure 10

Summary of dissolved oxygen deficit compared to background (upstream) conditions for commercial net pens in prior studies. N = 12.

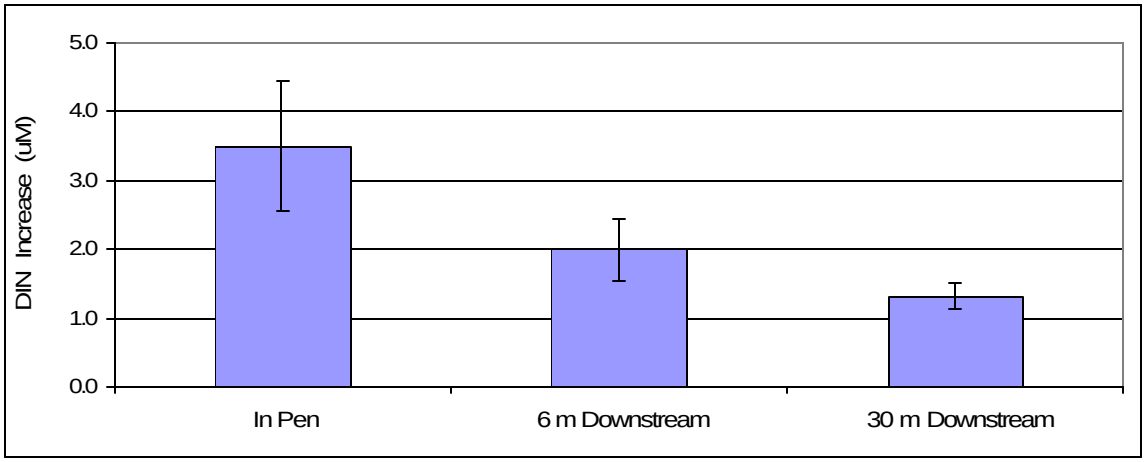

Figure 11. Summary of dissolved inorganic nitrogen increases inside commercial net pens and immediately downstream relative to ambient conditions as described in text. N = 12.

6. Description of Puerto Rico Fish Farm Site and Operation

6.1 Location and Site Layout

Here we describe the proposed farm site, its location, dimensions of pens, production zone (sediment impact zone) size and configuration as designated by the Puerto Rican Environmental Quality Board, and other factors used in our modeling. Ocean Harvest Aquaculture has previously submitted various planning and support documents to EPA and other agencies and herein we use the same information unless otherwise noted and make no attempt to include all the related information. Figure 12 and Table 4 describe the corner locations for the overall mixing zone shown as the inner, orange box in Figure 13. The zone closely approximates a square, but not exactly, as previously determined through the Puerto Rico Environmental Quality Board, Water Quality Certificate where it is designated as the "production" zone.

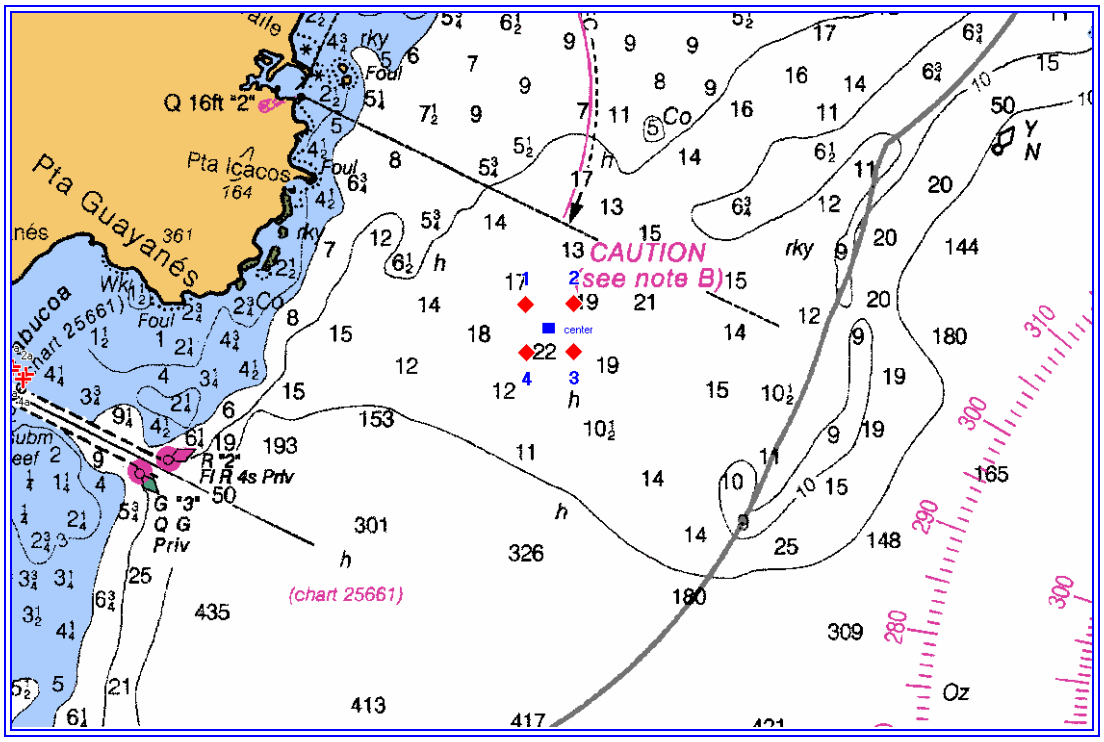

Figure 12. Location of production zone corners of approximately 500 x 500 m dimension.

Pens would occupy less than 2.2% of this area shown within the red diamond icons.

Table 4. Summary of proposed fish production zone corners.

Corner or Location	Latitude	Longitude
1	N 18°03'25.9"	W 65°46'24.5"
2	N 18°03'26.2"	W 65°46'07.5"
3	N 18°03'09.9"	W 65°46'07.3"
4	N 18°03'09.69"	W 65°46'24.3"
Center	N 18°03'17.9"	W 65°46'15.9"

Table 5 includes proposed and modeled dimensions and values necessary for the modeling process.

Table 5. Proposed site: planning and modeled characteristics.

Characteristic or Parameter	Actual or Modeled Value
Diameter & footprint area of single cage	26.5 m Diameter; 551.5 m^2 plan view area
Cage type, Number of cages	SeaStation (submerged, bi-conical shape); 10 cages
Effective cage volume, each cage	2,700 m^3 (approximate)
Cage volume for all 10 cages	27,000 m^3 (approximate)
Modeled cage height	10 m (actual vertical height 15 m)
Site depth	33 m , 32 – 35 m extreme range
Modeled cage depth	Cage top 5 m below surface. 10 m deep effective cage height, maximum modeled depth therefore 15 m.
Overall production zone area	~ 500 x 500 m = 0.25 km^2
Modeled production zone area	0.244 km^2
Proposed cage array configuration	2 rows of 5 each, rectangular array, aligned perpendicular to prevailing current direction
Dimensions of 2 x 5 array: outside edge	181.8 x 372.5 m
Area of 2 x 5 cage array to outside edge	67,721 m^2
Single cage footprint area	Radius =13.25 m; Area = 3.14 x r^2 = 551.5 m^2
Area of all 10 cages consolidated into one rectangle for most conservative modeling purposes	5,515 m^2 = < 2.2% of production zone

Characteristic or Parameter	Actual or Modeled Value
Dimensions and volume of simulation single, composite cage	52.5m x 104.9m x 10 m deep = 55,062 m^3 ; 55,062/27,000 (true cage volume) = 2.04 so modeling density reduced by ½ to achieve ~15 kg m^{-3} peak loading
Entire Modeling domain	2.7 km x 3.3 km = 8.9 km^2

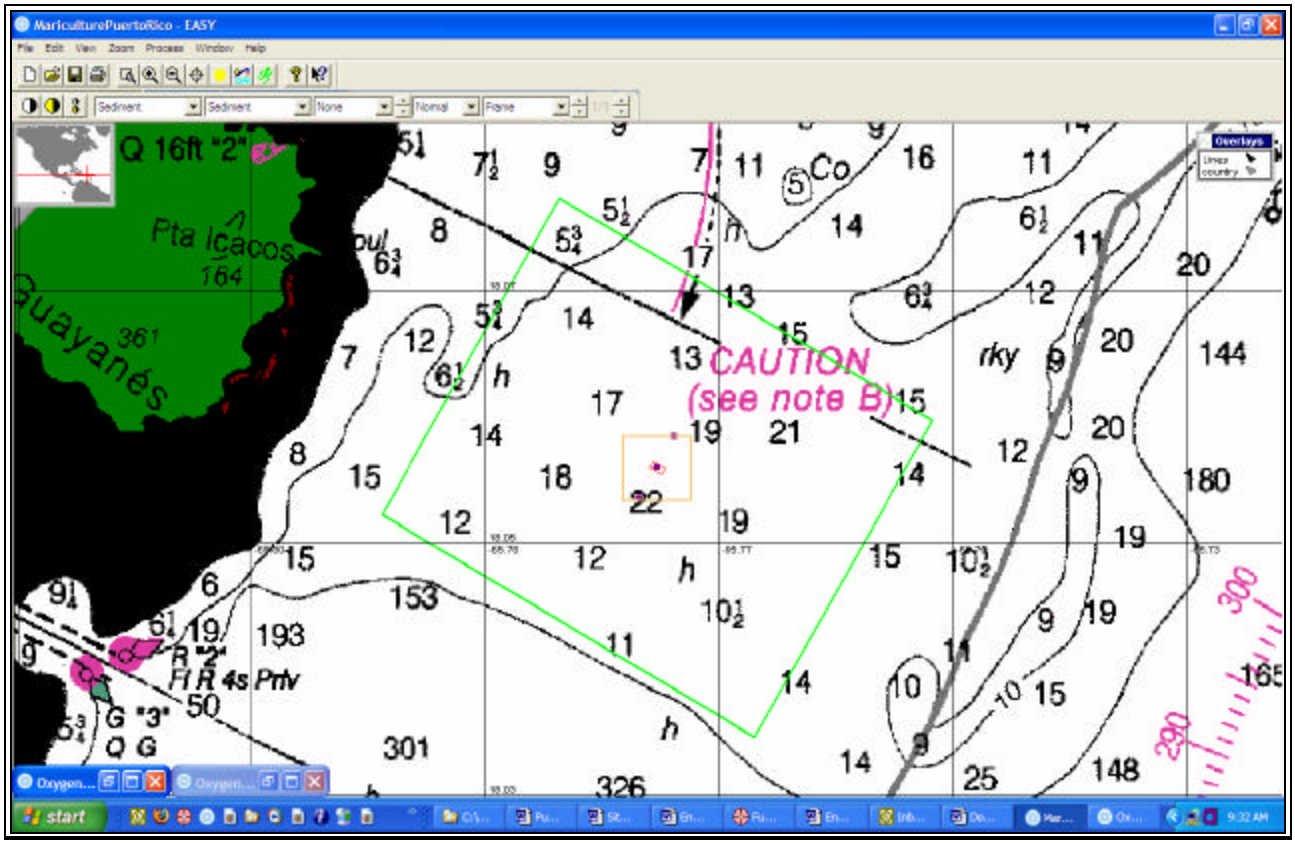

Figure 13. Bathymetric map of large modeling domain (green box), production zone (orange intermediate-sized box) and modeled pen area (inner red rectangular box in center).

6.2 Hydrographic Characteristics of Site

Table 6 summarizes the expected range of pertinent, ambient hydrographic parameters used in modeling the site with the expected mean value for each. For more details about each parameter, see the specific source document cited in the table. Figure 14 illustrates current vectors about the compass rose for the first current meter record that mostly shows wide variation of current direction from West through south to east directions.

Table 6. Background, ambient hydrographic, physical and sediment characteristics of proposed site and vicinity.

Parameter	Values	Source
Water Temperature	27 – 29 °C	Mercado et al. 1996; Capella et al. 2003, Alston et al. 2005,
Salinity	34 – 36.3 psu	Mercado et al. 1996; Capella et al. 2003, Alston et al. 2005
Mixed layer depth, seasonal thermocline	To bottom at site at all times except 25 m in fall	Capella et al. 2003
Dissolved inorganic nitrogen concentration	0.1 µM mean	Mercado et al. 1996, unpublished OTEC data from J. Capella (pers. comm., Excel data files)
Dissolved Oxygen concentrations	4 – 7 mg L^{-1}	Alston et al. 2005
Chlorophyll *a* pigment concentrations	0.1 µg/L mean	Unpublished OTEC data, pers. comm. J. Capella
Background sediment total organic carbon in general	0.3 to 0.8 percent	Morelock et al. 1994
Sediment characteristics at proposed site	Mostly hard sand with sparse algal, soft coral and/or	Capella 2004
Mean current velocity from fixed point current meter	Record 1: 8.5 cm sec^{-1} Record 2: 10.3 cm sec^{-1}	Capella 2004a, 54 d time series Capella 2004b, 104 d time series
Current velocity 90th percentile value	15.1 cm sec^{-1} 18.9 cm sec^{-1}	Capella 2004a Capella 2004b
Mean flow vector & speed	Record 1: to SE, 154°T Record 2: to NE, 320°T	Capella 2004a Capella 2004b
Typical strong velocity value of meter records	~ 20 cm sec^{-1}	Capella 2004a
Maximum current velocity recorded, fixed meter	Record 1: 32.6 cm sec^{-1} Record 2: 52.9 cm sec^{-1}	Capella 2004a Capella 2004b
Degree of current direction variability	Large, indicated by low R/S ratio (index of flow unidirectionality) of 0.35 and 0.27 for each record	Capella 2004a Capella 2004b
Acoustic Doppler Current Profiler Results, spring tides	Stronger than expected with mean velocity about 30-40 cm sec^{-1}, no differences with greater depth	Rensel unpublished ADCP results, 19-20 Oct 2005 transects about 1 km long through site

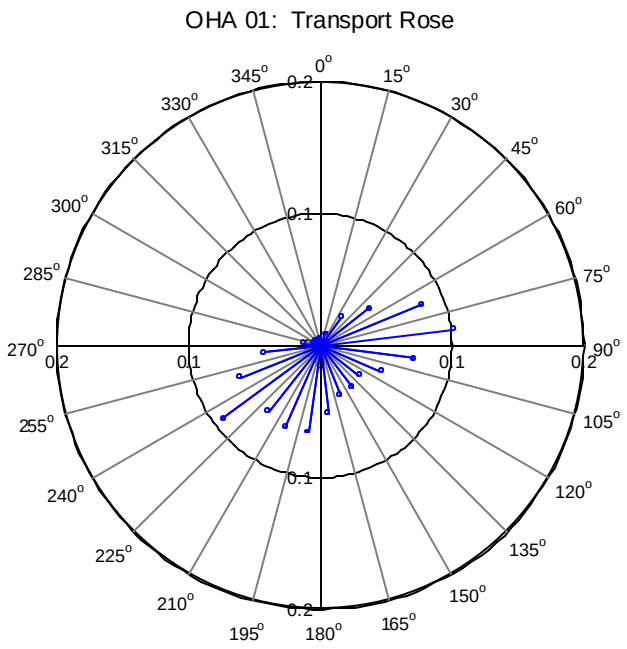

Figure 14. Current vector rose from Capella 2004a.

6.3 Additional Studies of Site Characteristics

In addition to the fixed current meter studies cited above, we conducted analysis of current velocity throughout the general area of the proposed fish farm on 18 and 19 October 2005 using an Acoustic Doppler Current Profiler (ADCP, 300 MHz RDI sentinel, downward profiling, small boat mounted). We surveyed ~ 2 km length transects North/South and East/West through the proposed project area in the channel between Humacao, Puerto Rico and Vieques Island. The goals of this work were to determine optimal siting in terms of depth and velocity and to investigate the strength of water currents throughout the water column including near bottom.

The data indicates that the proposed site is not substantially different from other areas within about a 2 km area. A typical example of this is shown in Figures 15 and 16 of a north to south transect showing current velocity approximately constants throughout the water column in all locations. Wind waves were relatively high during the study which resulted in unusually large amount of blank cells in the results, shown as the white area. Enough data was collected to verify that most velocity results were at least > 20 cm sec^{-1} as noted in Table 6. This study was conducted during a spring tide series; hence the velocity values were greater than the fixed current meter records of Capella (2004a, 2004b).

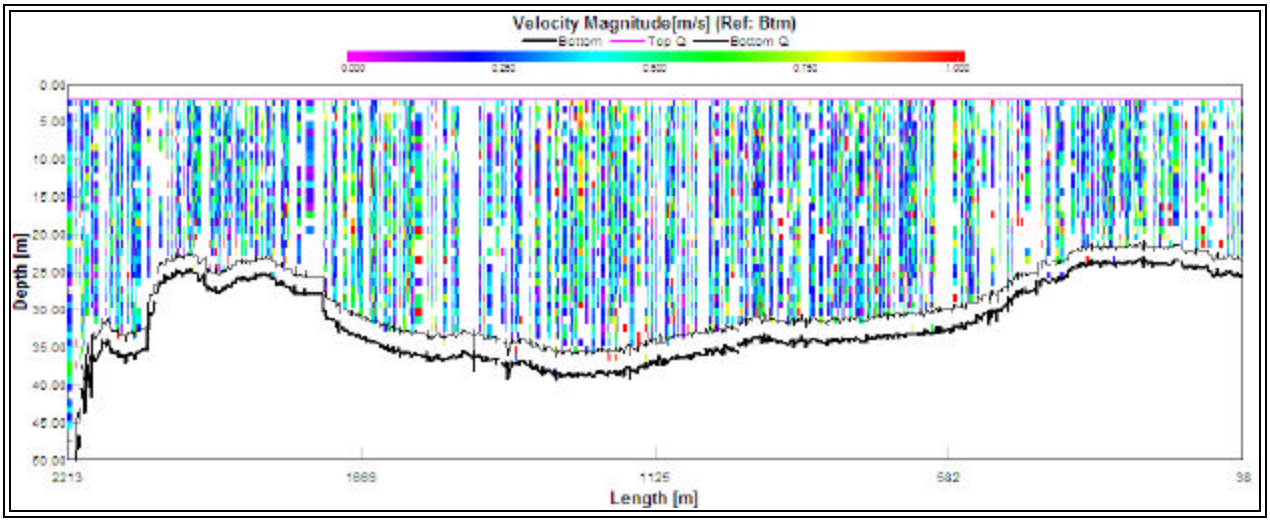

Figure 15. North (right) to South (left) transect of velocity magnitude through proposed net pen farm site from October 20, 2005 (transect 94) as an example of typical results of the ADCP study.

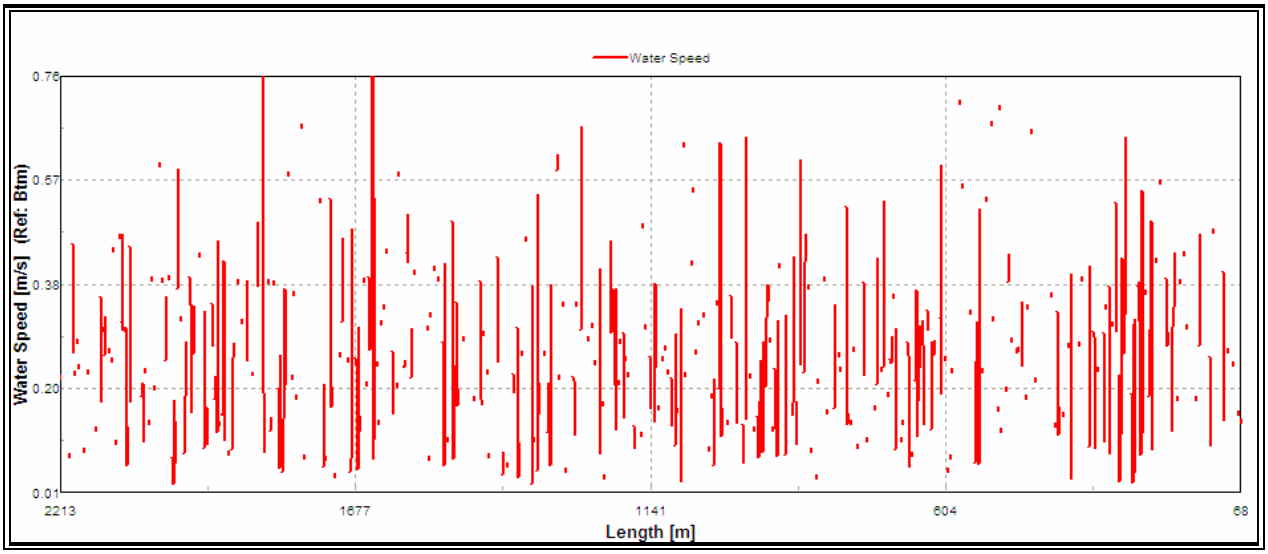

Figure 16. North (right) to South (left) transect of range of velocity through proposed net pen farm site from October 20, 2005 (transect 94) as an example of typical results of the ADCP study. X axis ranges from zero to 0.76 m sec^{-1} (76 cm sec^{-1}).

Current velocity was relatively strong throughout the water column with very little apparent attenuation at depth. Such conditions are desirable for sustainable, long term maintenance of sea bottom conditions, for example, maintenance of aerobic conditions of surficial sediments, resuspension and saltation of particulates to expedite transport, respiration and assimilation of waste carbon and solids.

Mean velocity of several hundred ensembles (groups of data collected from individual vertical profile "pings") of data are plotted versus direction in Figure 17. This is another means to summarize randomly selected portions of the same data shown above. Again, the current velocity shown here are ideal for sustainable net pen aquaculture and stronger than desirable for a long term mean, but since the data was collected during spring tides, lesser long term mean velocity would be expected. Mean velocity in this Figure was 39.4 cm sec^{-1} (SD 12.7) and 23 sets of three contiguous vertical profiles (ensembles) were analyzed over the entire transect. The direction component of data shows a mean direction of 152° True (SD 40.5°T) for this relatively short time period.

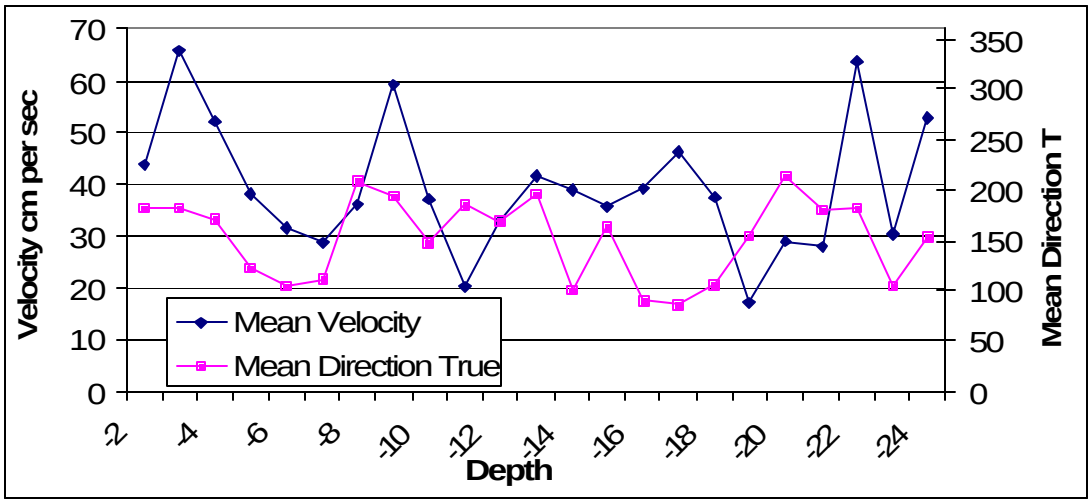

Figure 17. Example of acoustic Doppler current profiler data from transect through the proposed site on 19-20 October 2005.

6.4 Fish Culture Characteristics

Table 7 summarizes characteristic of the fish culture plan.

Table 7. Proposed site: Fish culture characteristics.

Characteristic or Parameter	Actual or Modeled Value
Fish stocking size and timing	10 gram in March
Size at harvest and timing	4.5 kg average, October through December
Average growth rate	~ 700 grams per month
Specific growth rate	~ 0.07 declining to 0.01 at end of cycle commensurate with increasing size and von Bertalanffy growth function
von Bertalanffy growth constant k	Growth constant of 0.65 with units of reciprocal time (e.g., year $^{-1}$) from FishBase
Fallow period (no fish in water)	~ Mid January to beginning of March
Maximum density of fish at harvest to maintain health	15 kg m^{-3}
Fish mortality, annualized	10%
Maximum feeding rate	Varies with fish size from 7% to <2% d^{-1}, see text.
Feed use per year	At 3% loss, 1.2 Food Conversion Ratio = 556,200 kg/yr
Feed moisture content	~ 8%
Feed C & N composition	Carbon 0.44, Nitrogen 0.07
Fecal settling rate	1 cm s^{-1} See section 7.1 for discussion.

7. Other Model Coefficients

The following coefficients were evaluated and used in the model; several were varied in the sensitivity analysis as explained later.

7.1 Fish fecal Settling Rates

Fecal settling rates for salmonids dominate the literature but these are not appropriate for marine fish. Findlay and Watling (1994), Elberizon and Kelly (1998), Panchang et al. (1997), Chen et al.

(1999) all examined settling rates of salmon feces, from small (25g) to relatively large (1kg) fish. The mean settling rates varied from 2 to 6 cm s^{-1} and rate was related to fish size as expected. Cromey et al. (2002a) examined fecal pellets from even larger fish (*Salmo salar)* of 3.4 kg mean weight, and found settling rates averaging 3.2 cm s^{-1}.

Marine fish fecal settling rates are scarcer, but perhaps of higher quality. With the exception of Japanese *Seriola quinqueradiata* (Japanese yellowtail, Iikura 1974, 5 cm s^{-1} but likely large fish) marine species studied had diffuse, slowly sinking fecal matter. Shona Magill and Chris Cromey and their colleagues (in press) in Scotland and in the Mediterranean Sea area have done most of this marine fish fecal settling work, focusing on gilthead sea bream, *Sparus aurata,* and sea bass *Dicentrarchus labrax*, that are raised in pens in the Mediterranean Sea. They collected fecal matter from sediment traps suspended below net pens for 2.5 to 6.75 hours and transferred the contents to the laboratory for resuspension in 2 m high Plexiglas cylinders. Using advanced but laborious video tracking methods applied to over 1000 particles for each species, they found mean settling rates of 0.70 and 0.48 cm s^{-1} for sea bass and sea bream fecal matter respectively.

Settling rates for cobia feces are not known, but anecdotal evidence from hatchery and university operations indicate fecal matter of fluffy, light composition, as would be expected for marine fish of the size being evaluated here. Accordingly, we select a conservative (faster than observed for sea bream and sea bass) value of 1.0 cm s^{-1}.

7.2 Resuspension Rates

In recent years several studies have indicated that resuspension and transport of fish farm wastes are among the key factors to understand in modeling the effects of fish farms on sediments (Panchang et al. 1997, Cromey et al. 2002a, 2002b, Riedel and Bridger 2003).

At less than a given, species-specific current velocity, fish fecal and food wastes will settle to bottom and remain in the same location, which is termed a “depositional “ condition.

At higher rates of flow, wastes are resuspended and hop, skip and move across the bottom until current velocity decreases again. This often occurs in “erosional” conditions and of course there is a continuum between the two extremes that we term “transitional” conditions. Most modern fish farms are located in these transitional conditions and as long as the sediments do not remain on the bottom for extended periods (i.e., days), the recently deposited sediments are subject to being resuspended and transported in the process of “saltation” which is defined as particles hopping and skipping across the bottom. In this process, particles are eroded into smaller sized particles and more easily moved and are of course available to the food web for assimilation. Presently AquaModel is designed to simulate transitional or erosional sites with stronger current velocities as there is no consolidation factor. We could add one, but we prefer to design around sites that are more sustainable that do not include depositional sites.

The best estimate of resuspension rate for salmonid wastes is 9.5 cm s^{-1} as measured or modeled 2 m above the bottom (Cromey et al. 2002a, 2002b, Cromey and Black in press). Yet we know that salmon fecal matter is much denser and cohesive than most marine fish, so that rate is not appropriate for cobia. We selected a rate of 6.0 cm s^{-1} for most of our model runs, but varied it up and down to see the effect. As shown later, it has a major effect but even at the salmonid rate of

9.5 cm s^{-1} there would not be detectable amounts of carbon deposited on the bottom at the edge of the mixing zone and a relatively low mean value for directly under the cages.

7.3 Carbon oxidation rates

Another important factor in modeling fish farm effects is the rate at which carbon deposited on, or moving along the bottom is oxidized by bacteria or assimilated by the food web. The rate of organic matter degradation by microorganisms is often estimated using a first order kinetics or a Michaelis-Menton kinetics approach with similar result in cases where substrate, instead of microbial biomass, is limiting. When a fish farm begins operating at a new site, the biomass of microorganisms on and in the sediments beneath and immediately adjacent to it will increase in abundance commensurate with the increase in organic matter provided by the farm. Within reasonable bounds, after the farm operates for some period of time the microbial biomass (and macrofauna too) approximate a steady state to process the wastes. Beyond reasonable bounds, if too much carbon is deposited, sediment bacterial communities shift to anaerobic (sulfide reducing) which tends to extirpate many sensitive invertebrate macroinvertebrates, infauna or epifauna. Generally, less than about 1 to 1.5 percent total organic carbon distributed through the top 2 cm will not result in the shift to anaerobic conditions, depending on sediment grain size and water temperature. Here we deal with the carbon added to be added by the fish culture operation, keeping in mind background levels of TOC that are relatively low, approximately 0.5 percent. Total carbon levels are much higher but most of this carbon is locked up as biogenic, refractive carbonates from shell and coral.

Tlusty et al. (2000) demonstrated that fish fecal matter had a very high solubility potential, loosing approximately 50% of its organic matter in 12 day exposures to water flow. Fish feces are thus "non-refractile" forms of carbon, unlike carbon more tightly locked up in refractile forms such as tree trunks or bark or carbonate carbon such as shell.

Prior modelers of fish farm carbon oxidation rates (Fox 1991, Pachang et al. 1993) have often used the value of 1 percent per day, which stems from an EPA (1982) document dealing with sewage sludge oxidation. The reaction is temperature dependent and likely faster in the warm waters of Puerto Rico. .

Hendrichs and Doyle (1986) found carbon in phytoplankton cells (*Cyclotella* diatom) decomposed at rates > 0.14 per day (1.4% per day), but that was for a mean temperature of 7°C. Allowing for two doubling due to Q10 effects to get us up to 28°C increases it by at least a factor of 3 (0.42 per day).

Fujii et al. 2003 found carbon decomposition rates for *Skeletonema* of 0.13 day/day at 20°C and semi-refractory carbon in the form of POC at 0.008 per day, both at 20°C.

Given the above, we conservatively choose to use 1.0% per day and experimentally varied the rate later in the sensitivity analysis. As discussed below, this is probably an extremely conservative choice, and in the near future we expect to see more studies and literature focused on this topic.

8. Modeling Results

8.1 Case 1: Probable Effects Scenario

We quantitatively evaluated conditions at the pen site and at the boundaries where the plume from the fish farm was most likely to occur. Based upon current meter records, we selected a cell along the north boundary and another on the south boundary to export data to a spreadsheet for a 28 day lunar cycle period for every 5 minute period. This resulted in a total of 8,064 sets of calculations for each parameter. These two locations represent worst-case positions to evaluate effects that could occur outside the mixing area.

Case 1 was constructed to be a worst case whenever possible in terms of:

Fish biomass and density: We selected the largest size (4.5 kg) and largest density (15 kg/m3) expected for operations. In fact the simulation began with the largest fish and by the end of the simulation the total biomass within the farms exceed the maximum expect by 35%.

Current Velocity: We used the first set of current meter data collected by Capella (2004a) which had slightly lower velocity than the second set. Slower velocities - tend to concentrate effects near the cages. Only the first 28 days of the current meter record were used with a mean velocity of 8.4 cm s^{-1}. The full record averaged 8.5 cm s^{-1} ,which was 1.7 cm s^{-1} slower than the second record. The second full record averaged 10.3 cm s^{-1}.

Pen Configuration: For the purposes of modeling, we combined the ten separate cages into one - pen, greatly concentrating - impact in that area. This greatly overstates the effect on all the simulated parameters, particularly sediment carbon.

No Fallow Period Effect: The simulation did not involve the annual period of time from January through early spring during which the cages will be empty. As has been shown repeatedly in other studies The sea bottom will rapidly recover from any effects during this time period, .

Feed Rates: We purposely set feeding rate at 4% of body carbon per day, which is very high for the size of cobia modeled in most of our simulations (4.5 kg). In Taiwan, Liao (2004) reports only 0.5 to 0.7% of body weight per day, but Riedel and Bridger (2003) modeled cobia with a 4% value and no stated rationale. Feed rate of cultured fish decreases with increasing body size, but we are uncertain of the size of the decrease for cobia growing in waters that remain optimally warm all year. Based on our calculations, the feed rate should be ~ 2% per day at the 4.5 kg size. AquaModel shunts excess feed beyond the ability of the fish to consume into the waste feed category and it is calculated as loss to the bottom. In part feed rate was set very high to offset the settling rate of waste feed, which in AquaModel is presently limited to the same rate as waste feces, at 1 cms^{-1}. Waste feed is much richer in carbon than feces by a factor of 3, so the doubling of waste feed conservatively increased carbon waste rates far beyond what would exist in a normal, modern fish farm operation.

Background Conditions: We used the best regional and local literature values for all the other factors in the model including water temperature, salinity, dissolved oxygen, dissolved inorganic

nitrogen, current velocity and direction, etc. as previously illustrated in the tables above. Physical parameters such as fish fecal matter settling rate and resuspension rate were assigned the optimum values previously discussed.

Background sediment carbon was set at zero to assess only that portion to be added by the proposed fish farm operation. It is emphasized that the values expressed here for sediment carbon are not to be compared directly to those found in field work. The carbon added by the pens to the bottom will initially be restricted to the surface layer. Total organic carbon sampling usually involves coring into the bottom to a widely accepted depth of 2.0 cm (EPA-PSEP 1997). Our calculations indicates that waste carbon from the farm will be diluted by a factor of 100x for an addition of 1 gram per m^2.

A time series of screen prints from Case 1 simulation showing low and high velocity time periods is shown in Figures 18 through 21. For these Figures, the model display was set to show carbon deposition, which is indicated by white (no carbon) or faint green color indicating very low (<0.1 g C m^{-2}) values for areas outside the composite cage system. The numerical results of the simulation are shown below in Table 8 for the pen site and areas of the north and south mixing zone boundaries, the latter most likely to be influenced by the farm.

Table 8. Results of case 1 probable effects simulation at three locations, 1) within or under the cage, 2) at the south mixing zone boundary, 3) at the north mixing zone boundary.

Change refers to change from background conditions, previously stated. Sediment C must be divided by 100 to estimate concentration within the top 2 cm, a standard regulatory coring depth for aquaculture and most biological studies (EPA-PSEP 1997).

Within or Under Cage	**Flow Velocity**	**Growth Rate**	**Fish Biomass**	**Dissolved Oxygen**	**Nitrogen**	**Phytoplankton**	**Zooplankton**	**Fecal Carbon**	**Feed Carbon**	**Sediment Carbon**
Units→	cm s^{-1}	1/d	MT	mg L^{-1}	µM	µg L^{-1}	µg L^{-1}	g m^{-3}	g m^{-3}	g m^{-2}
Mean	8.4	0.01	483.9	5.47	1.06	0.06	0.09	0.02	0.06	0.75
SD	5.2	0.00	421.7	0.18	0.71	0.03	0.02	0.04	0.03	1.51
Change	na	na	na	-0.23	+0.91	-0.04	+0.04	+0.02	+0.06	+0.75
90th %	15.9	0.01	543.4	5.63	1.96	0.10	0.13	0.03	0.10	2.82
10th %	2.9	0.01	426.5	5.24	0.42	0.03	0.06	0.01	0.03	0.00

South Mixing Zone Boundary	**Dissolved Oxygen**	**Nitrogen (DIN)**	**Phytoplankton**	**Zooplankton**	**Fecal Carbon**	**Feed Carbon**	**Sediment Carbon**
Units →	mg/L	µM	µg L^{-1}	µg L^{-1}	g m^{-3}	g m^{-3}	g m^{-2}
Mean	5.70	0.16	0.06	0.09	0.00	0.00	0.02
SD	0.01	0.03	0.03	0.02	0.00	0.00	0.05
Change	0	+0.01	-0.04	+0.04	0	0	+0.02
90th %	5.71	0.19	0.10	0.13	0.00	0.00	0.09
10th %	5.69	0.10	0.03	0.06	0.00	0.00	0.00

North Mixing Zone Boundary	**Dissolved Oxygen**	**Nitrogen (DIN)**	**Phytoplankton**	**Zooplankton**	**Fecal Carbon**	**Feed Carbon**	**Sediment Carbon**
Units	mg L^{-1}	µM	µg L^{-1}	µg L^{-1}	g m^{-3}	g m^{-3}	g m^{-2}
Mean	5.70	0.01	0.06	0.09	0.00	0.00	0.00
SD	0.01	0.00	0.03	0.02	0.00	0.00	0.01
Change	0	+0.01	-0.04	+0.04	0	0	0
90th %	5.71	0.01	0.10	0.13	0.00	0.00	0.00
10th %	5.69	0.01	0.03	0.06	0.00	0.00	0.00

Table footnotes: Nitrogen units are micomolar (µM = µg at./L). 1 uM DIN = 14 ug/L = 14 ppb = 0.014 mg/L N and refer to nitrate+nitrite+ammonia, or DIN for short. North or South refer to the capture cell along the north or south mixing zone boundary. Pen refers to within the fish cage.

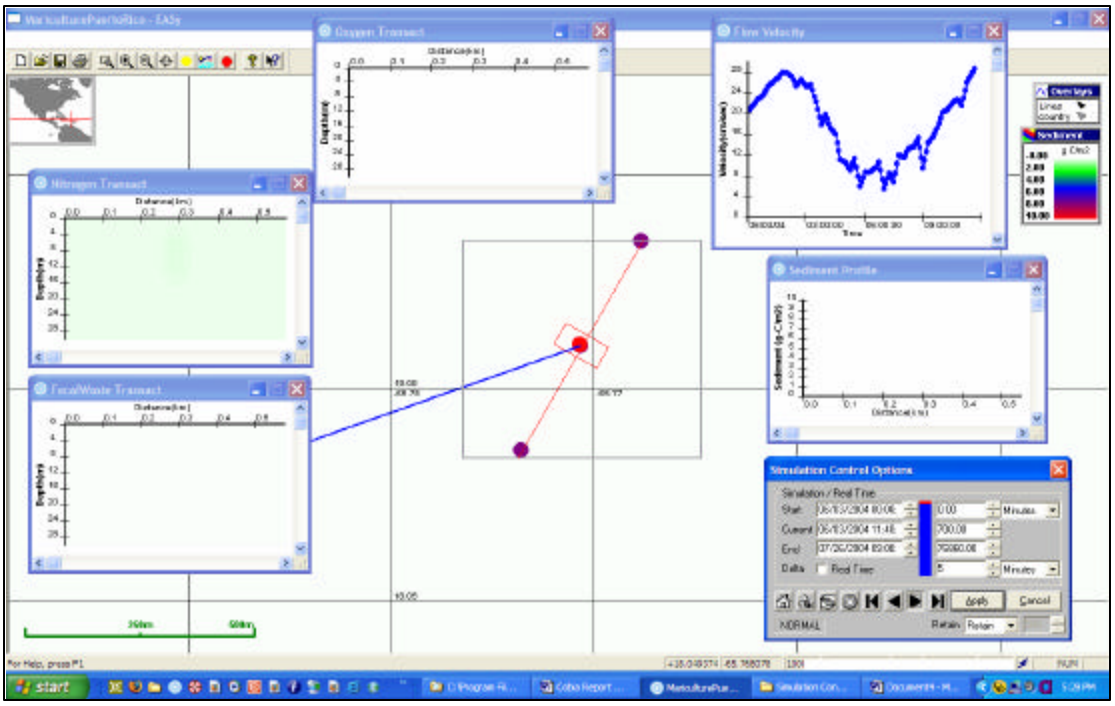

Figure 18. Typical higher current velocity screen print.

Top right velocity plot at 28 cm s^{-1}; no carbon being deposited on bottom (right center plot) and very slight localized nitrogen plume along center of transect (left center plot). Blue line from center is a current vector (speed and direction) indicator.

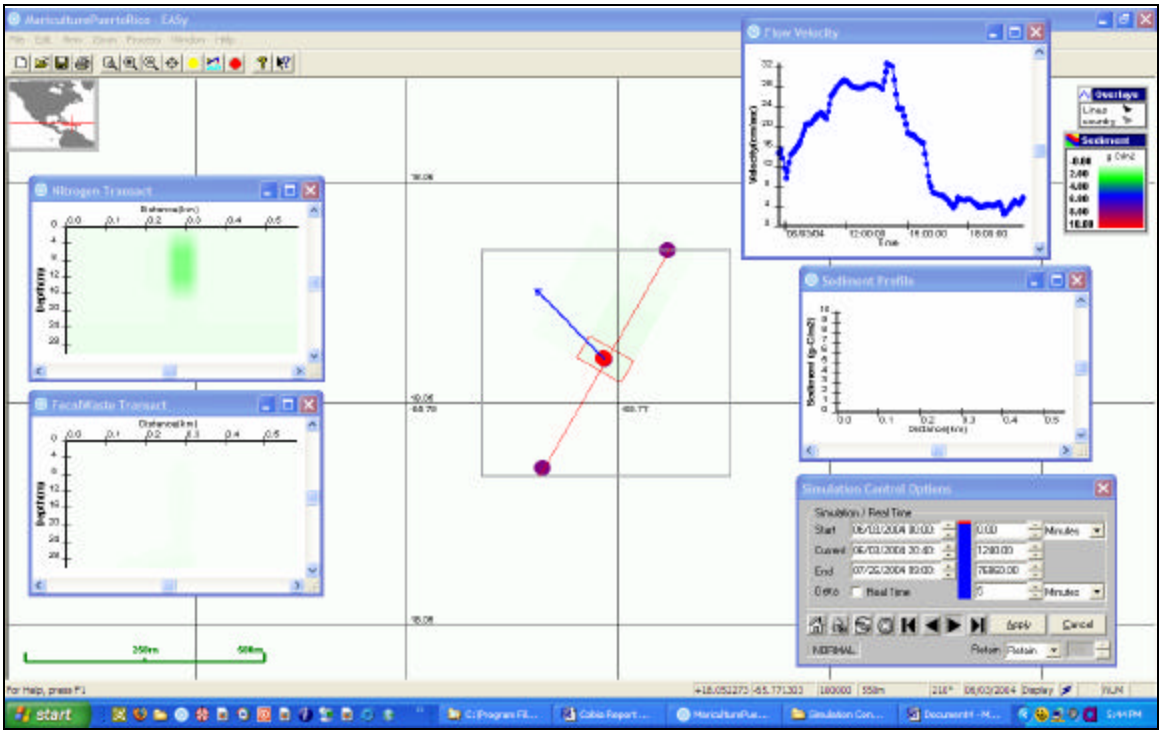

Figure 19. Later in same time series after a sustained period of slow velocity

Note faint shadow to NE indicating low level <0.2 g C/m2 deposition graded toward edge of mixing zone.

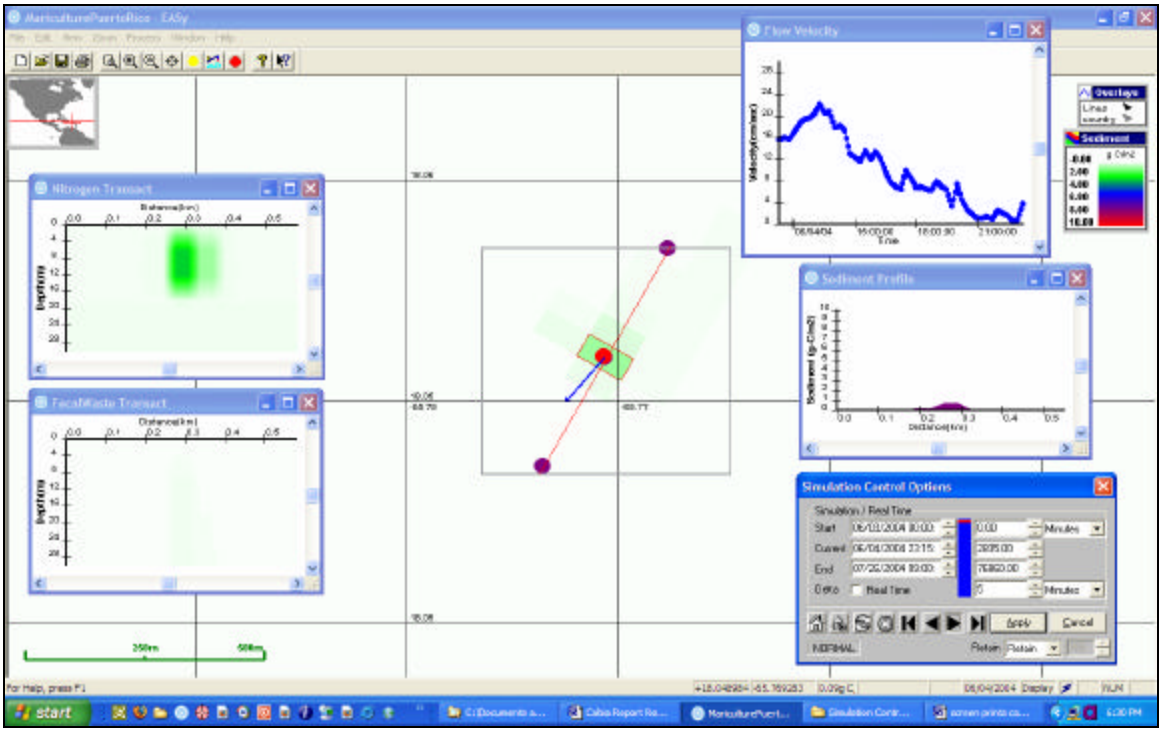

Figure 20. Much later in same time series with current direction reversal and maximum carbon deposition showing in main plot and in profile in right center (scale 1 to 10, purple mound indicating < 1 g C m^{-2} beneath simulated cage.

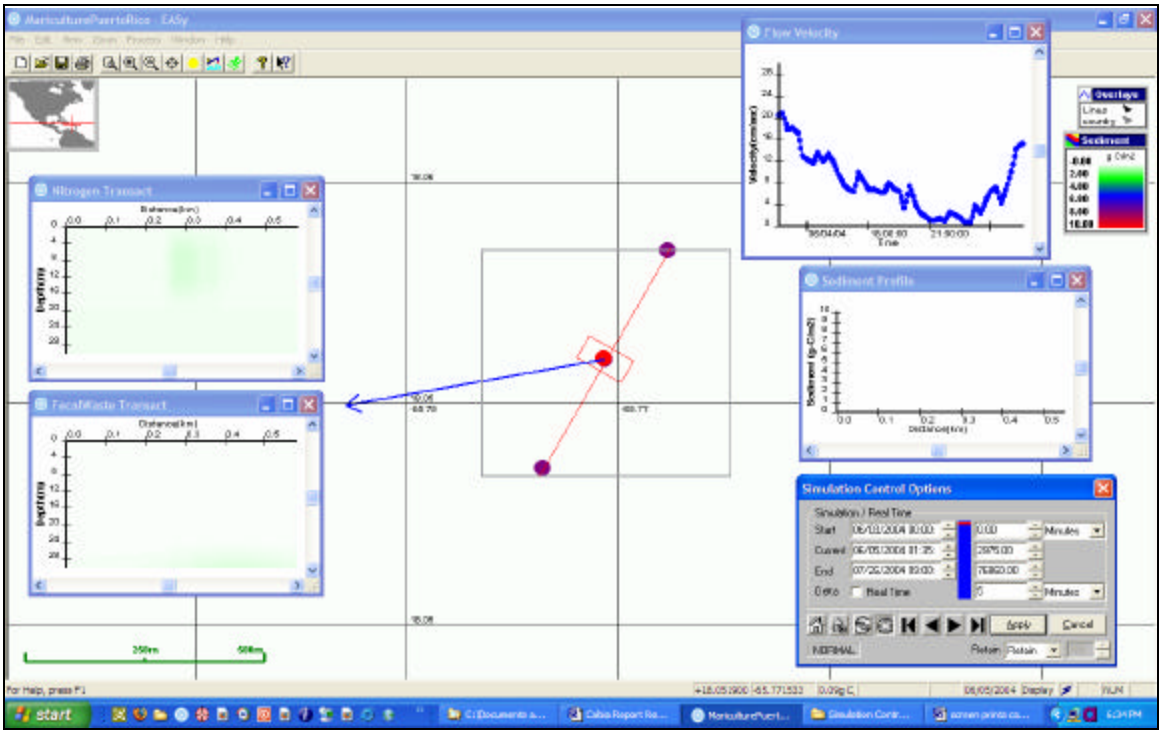

Figure 21. Stronger currents resuming and resuspension having removed temporarily deposited solids from the bottom.

In Figures 18 to 21 we show the output display with only a few plots showing. AquaModel has the ability to show many different plots simultaneously and the user may select one of about 10 different main scene settings. Here we only show the main scene set to show carbon deposition.

Case 1 simulation results indicate that effects of the farm will not be detectable for any of the water or sediment quality parameters at the edge of the mixing (production) zone. This is what we would have expected, based on extensive experience with other fish grown in net pens including marine fish in Hawaii (Ostrowski et al. 2001, C. Helsley, pers. comm.).

Sediment Carbon: As expected, there will be some minor increase in carbon directly beneath the cages, but again, the simulation is based on one composite cage, not the 10 individual cages that will be spaced throughout a much larger area within the production zone. The model predicts a mean TOC concentration of 0.75 g C m^{-2} beneath the fish farm after a 28 day lunar tidal cycle. The model does not include a compaction or consolidation factor as it was judged not needed in the present case of a transitional to erosional seabottom.

The value of 0.75 g C m^{-2} when measured in a 2 cm deep core and homogenized in the laboratory would reduce the aquaculture carbon contribution to about 0.08 g C m^{-2}, a very low level. Compared to ambient conditions in Puerto Rican marine waters, this means an increase of about 12% from 0.5 to 0.58 g C m^{-2}, which will diminish rapidly with distance from the cages within a few tens of meters. Even in much colder temperate waters, carbon deposition rates < 1 g C m^{-2} are not considered excessive and will not necessarily result in anaerobic surficial sediments (Hargrave, 1994).

Dissolved Oxygen: Dissolved oxygen within the composite cage system averaged 0.25 mg/L less than the ambient and modeling boundary zone concentration. This is typically what has seen for salmonid culture systems of comparable size and fish density. No reduction of dissolved oxygen is predicted at the edge of the mixing zone or anywhere close to it.

Repeated measurements by several authors (Normandeau Associates and Battelle 2003, Parametrix 1990, EAO 1997) have shown that deficits in the concentration of dissolved oxygen within the cages disappear within 5 to 30 m of even very large salmon cages. One of use (JER) has conducted many of these surveys (Parametrix 1990 and unpublished NPDES monitoring results). Our model has the capability of recording effects at any point within the modeling domain, but we focused on the edge of the mixing zone for regulatory purposes.

Phytoplankton and Zooplankton: Relatively low values were observed for phytoplankton throughout the modeling domain, which was expected, given the extent of dilution and the time period for added nutrient to be incorporated into cell tissue of phytoplankton (doubling rates of about a day). The reports of elevated phytoplankton biomass around fish farms was reported decades ago in Scottish sea lochs where current velocity was very low and flushing rates essentially nil (Richard Gowen, unpublished technical reports, Dunstaffnage Marine Laboratory, Scotland).

9. Sensitivity Analysis

Several dozen other runs of the model were conducted to assess the effects of key variables that were systematically altered around the values selected for Case 1, described above. Initial runs to arrive at the selection of Case 1 are not reported here but details of the runs with greater or lesser values than used in Case 1 are given in Appendix A as summarized here. In each case the reader may compare results for the variable change relative to Case 1.

9.1 Fish Density and Resulting Biomass

This factor was varied from 7.5 to 22.5 kg m^{-3} around the maximum planned fish density of 15 kg m^{-3} that will occur only for short periods prior to harvest. The mean simulation biomass during the 28 d runs for Cases 4 and 5 was 257 MT to 729 MT, respectively, compared to the mean of Case 1 at 484 MT. These modeling runs produced significant changes in results within the fish cages for dissolved oxygen, nitrogen and waste organic carbon deposition on the seafloor. However, no significant or measurable changes would be seen at the edge of the mixing zone. The lower density run indicated relatively low mean carbon sediment concentration on the seafloor, and the higher value produced a mean value of 1.5 g C m^{-3} which is near the threshold at which adverse effects would be noted directly under the cages (but not at a distance of a few tens of meters).

An additional run at 30 kg m^{-3} fish density was conducted in an attempt to stimulate a virtual phytoplankton bloom (Case 8, discussed below). This highest density, which is double the proposed density near harvesting time, would produce severe sediment carbon effects directly beneath the single, large composite-simulated cage but actual effects from the 10 separate cages would be much less. After scaling for the mixing of waste carbon with the ambient carbon in a 2 cm deep core yielded an average value of ~ 7.0 g C m^{-2} of sediment total organic carbon.. Such a value has been exceeded at other study sites, but is definitely to be avoided. Despite this elevated level, at the edge of the mixing zone the effects would not be measurable, with an estimated mean total organic carbon concentration due to the fish cage of 0.007 g C m^{-2}, assuming the sampler provides a 2 cm core that EPA often recommends.

9.2 Horizontal Turbulence

Horizontal dispersion was varied from a factor of 0.05 to 2.0 around the selected value of 1.0. The effect of this change was to decrease or increase lateral flow to simulate eddy diffusion and dispersion. These alterations produced a small change in the results for dissolved oxygen, nitrogen and sediment carbon deposition, but were less than the effect of fish density changes discussed above. See cases 6 and 7 of Appendix A.

9.3 Sediment Carbon Oxidation Rate

This was varied from 0.5 to 1.5% per day with no significant effects on mean carbon deposition beneath the cages. Advective current transport processes outweigh sediment carbon oxidation rates. This is a reasonable conclusion given the time scales involved (seconds versus days, respectively). See cases 2 and 3 of Appendix A.

9.4 Resuspension Rate

The threshold value for erosion of deposited waste was increased from the selected 6.0 cm s^{-1} to 7.7 or 9.5 cm s^{-1}. The latter is the value used in DEPOMOD for salmonid wastes that are significantly denser than marine fish wastes. The former (7.7) was merely half way between the selected rate and the salmonid rate.

Use of the salmonid value resulted in a significant sediment impact beneath the single, large simulated-composite cage with TOC averaging 7.3 g C m^{-2}. Use of the 7.7 cm s^{-1} rate resulted in half as much TOC beneath the same cage, with a mean value of 3.6 g C m^{-2}. In both cases the results were significant higher than the Case 1 projected result of 0.75 g C m^{-2}. A lower value was not used but may well be appropriate given the significant differences in waste density and size between salmonids and marine fish. See cases 10 and 11 of Appendix A.

9.5 Deposition Threshold

In this run we decreased the critical shear threshold water velocity at which waste particulates would begin to deposit on the bottom from 4.5 cm s^{-1} to 3.0 cm s^{-1}. This had the effect of reducing the mean sediment TOC beneath the fish farm by 55% from 0.75 g C m^{-2} to 0.34 g C m^{-2}.

This scenario may in fact be more likely than Case 1, due to the nature of marine fish fecal matter, but due to the uncertainty we retain the value of 4.5 cm s^{-1} selected in Case 1. The value of 4.5 cm s^{-1} was from salmonid waste modeling and likely was too high for cobia wastes.

9.6 Phytoplankton Bloom

In order to assess the possibility of a phytoplankton bloom or major effects on the plankton food web, we reduced the current velocity greatly in order to retain the waste nitrogen within the modeling domain. We reduced the mean velocity by a factor of 17 to a mean of 0.5 cm s^{-1}, maximum of 1.0 cm s^{-1} and to further enhance the chances we used a simple bi-directional current flow option of AquaModel. Concurrently, zooplankton density was varied in this process from 1.0 µg/L down to 0.1µg/L and even zero. Through an iterative process of several runs we were unable to stimulate a minor bloom until all zooplankton grazing biomass was removed. At that point, the biomass of phytoplankton increased to 0.25µg/L. This value of 0.25 µg/L, which is higher than the normal, mean concentrations by a factor of 2, but within the range occurring in Puerto Rican waters, and thus would not constitute a "bloom". For comparison, normal spring blooms in temperate northern waters may range anywhere from 5 to 30 µg L^{-1}. See Cases 8, 13 and 15 in Appendix A.

The inability to stimulate a bloom is not a deficiency of the model; it is more of a illustration of the effects of dilution and advection of cells that occurs in such offshore sites. By increasing the growth rate of phytoplankton well above 1 per day we could stimulate higher levels of chlorophyll *a* in the model domain, but such growth rates are unlikely. As discussed above, we had to greatly reduce current velocity and hold more than double the normal peak amount of fish to stimulate even a minor bloom.

10. Discussion

In general, AquaModel simulated effects within the range expected from studies of other fish farms of this size. AquaModel is rooted in existing models that have been validated and published but provides a unique, concurrent evaluation of both water column and benthic effects.

The primary case runs of AquaModel show modestly small effects within or under the simulated-composite cage but no measurable effects near the edge of the mixing zone (an area known as the "production zone" in the Puerto Rican Water Quality Certificate). As expected and seen with most modern commercial net pen farms, sediment carbon is deposited beneath the cages with flux rates controlled mostly by current velocity but not at distances of more than a few tens of meters from the perimeter. In cases where effects have been detected farther (e.g., Brooks 2003: subtle biological effects measured to about 150-200 m around several inshore fish farms in British Columbia) the mean current velocities or current frequency distribution were relatively slow (generally 3 to 5 cm s^{-1} in most cases) and current direction likely to be mostly bi-directional. Slow velocity and limited variation of direction act together to create a depositional environment that is less desirable for large-scale net-pen aquaculture.

There was some uncertainty about a few model coefficients for preparation of Cobia AquaModel, primarily because the culture of cobia is relatively new compared to other species that have been raised in net pens for decades and studied extensively. To deal with the uncertainties, we choose conservative or very conservative values for these coefficients. We also used other conservative approaches such as use of the slower of two current meter records. Despite these conservative factors, effects at the edge of the mixing (production) zone were projected to be nil or so small as to be undetectable from careful measurement or observation.

Current velocity at the proposed OHA farm site is slightly below optimal if we use the metric of mean current velocity in a bi-directional tidal channel, a situation often occurring in temperate water pens for salmon. But waste dispersion is a function of current direction too, and current direction at the OHA site is relatively great as measured and reported by Capella (2004a, 2004b). This is particularly important for limiting benthic impact and allows for additional dispersion and assimilation of carbon by the ecosystem.

Extensive studies of a pilot scale fish farm in Puerto Rico near the Island of Culebra have been performed (Alston et al. 2005) and include a wide variety of useful data and studies. But documentation available to us did not include incremental time-series feed use, fish growth or linkage to benthic effects in a quantitative sense, limiting the usefulness of that study to our modeling needs. Nevertheless, it is important to remember that these individual, submerged cages provide a more diffuse release of waste materials than can be achieved with steel surface cages that most large-scale commercial fish farmers worldwide presently use. In this case, OHA will further limit effects on the sea bottom by maintaining the cages as near to the surface as possible. The effects of current velocity, greater depth and variable direction will therefore enhance the ability of the marine ecosystem to assimilate particulate wastes that reach the bottom.

The sensitivity analysis we performed demonstrated the importance of resuspension as a factor that limits carbon deposition and allows for broad transport of waste particulates. This effect has

previously been demonstrated with a benthic model (DEPOMOD) using a fluorescent tracer in a situation where current velocity was significantly less than the OHA site (Cromey et al. 2002b, mean velocity 4.9 cm s^{-1}, maximum velocity 23 cm s^{-1}) and by other authors discussed herein.

The largest factor controlling water column and benthic effects was fish biomass (a function of fish density and size) and at the highest levels tested would produced significant and undoubtedly adverse effects, but these modeling results were only achieved by reducing the mean current velocity to about 20x less than the existing mean current. At proposed fish biomass levels, no significant adverse effects are projected even under the cages or nearby waters.

Future versions of AquaModel may allow modeling of individual cages or several groups of cages and allow variable feed sinking rates. The model is presently designed for use in transitional or erosive sea bottom environments but could be modified to include cumulative sedimentation effects as occur in slow current velocity sites. In this project we had the ability to capture modeling data at three points around the cages and on the bottom, which allowed us to simulate effects at the edge of the agency-approved mixing zone.

11. References Cited

Alexander, R.M. 1967. Functional Design in Fishes. Hutchinson University Library, London. 160 pp.

Alston, D.E., A. Cabarcas, J. Capella, D.D. Benetti, S. Keene-Meltzoff, J. Bonilla and R. Cortes. 2005. Environmental and Social Impact of Sustainable Offshore Cage Culture Production in Puerto Rican Waters. NOAA Federal Contract Number: NA16RG1611 Final report.

Bertalanffy, L. von 1938. A quantitative theory of organic growth (Inquiries on growth laws. II). Human Biol. 10: 181-213.

Bertalanffy, L. von 1960. Principles and theory of growth, pp 137-259. In Fundamental aspects of normal and malignant growth. W. W. Wowinski ed. Elseviers, Amsterdam.

Brooks, K. and C.V.W. Mahnken. 2003. Interactions of Atlantic salmon in the Pacific Northwest environment II: Organic Wastes. Fisheries Research. 62:255-293.

Capella, J.E., D.E. Alston, A. Cabarcas-Nunez, H. Quintero-Fonseca and R. Corstes-Maldonado. 2003. Oceanographic considerations for offshore aquaculture on the Puerto Rico-U.S. Virgin Island Platform. University of Puerto Rico Department of Marine Sciences. Pages 247-261 In C.J. Bridger and B.A. Costa-Pierce, Eds. World Aquaculture Society, Baton Rouge, Louisiana.

Capella, J.E. 2004a. OHA OOCA Studies Department of Marine Sciences UPR-RUM OHA1 Current Meter Deployment Report. Dated August 2, 2004. Aguadilla, PR.

Capella, J.E. 2004b. OHA OOCA Studies Department of Marine Sciences UPR-RUM OHA2 Current Meter Deployment Report. Dated Nov. 16, , 2004. Aguadilla, PR.

Chen et al. 1999 Physical characteristics of commercial pelleted Atlantic salmon feeds and consideration of implications for modeling of waste dispersion through sedimentation Aquaculture International **7:** 89–100.

Cromey, C.J. and K.D. Black (In press). Modelling the impacts of finfish aquaculture. Chapter 7 in: The Handbook of Environmental Chemistry. Environmental Effects of Marine Finfish Aquaculture. Volume 5: Water Pollution. Springer, Berlin Heidelberg New York.

Cromey, C.J., T.D. Nickell, and K.D. Black. 2002a. DEPOMOD - Modelling the deposition and biological effects of waste solids from marine cage farms. Aquaculture 214: 211-239.

Cromey, C. J., T.D. Nickell, K.D. Black, P.G. Provost, and C.R. Griffiths. 2002b. Validation of a fish farm waste resuspension model by use of a particulate tracer discharged from a point source in a coastal environment. Estuaries 25: 916-929.

Cromey, C.J. and K.D. Black (2005). Modeling the impacts of finfish aquaculture. Chapter 7 in: The Handbook of Environmental Chemistry. Environmental Effects of Marine Finfish Aquaculture. Volume 5: Water Pollution. Springer, Berlin Heidelberg New York.

Cromey, C. P. Provost, K. Black. 2003. Development of monitoring guidelines and modelling tools for environmental effects from Mediterranean aquaculture. Newsletter 2. Scottish Association for Marine Science Dunstaffnage Marine Laboratory, Oban, Argyll, PA34 4AD, Scotland, UK

EAO (Environmental Assessment Office). 1997. British Columbia salmon aquaculture review. Environmental Assessment Office, Government of British Columbia, 836 Yates Street,Victoria, BC V8V 1X4.
http://www.eao.gov.bc.ca/epic/output/html/deploy/epic_project_doc_list_20_r_com.html

EPA. 1982. Revised Section 301(h) Technical Support Document. Prepared by Tetra Tech. Inc. EPA Publication No. 430/9-82-011.

EPA-PSEP. 1997. Recommended guidelines for sampling marine sediment, water column, and tissue in Puget Sound. Puget Sound water quality action team report prepared for Puget Sound Estuary Program, U.S. Environmental Protection Agency, Region 10, Seattle, Washington. 47 pp. http://www.psat.wa.gov/Publications/protocols/protocol_pdfs/field.pdf

EPA 2002. EPA modeling QAPP Requirements for Research Model Development & Application Projects. On line recommendations for projects to receive EPA funding.

Elberizon, I.R., Kelly, L.A., 1998. Empirical measurements of parameters critical to modelling benthic impacts of freshwater salmonid cage aquaculture. Aquaculture Research 29:669– 677.

Findlay, RH, and L. Watling. 1997. Prediction of benthic impact for salmon net-pens based on the balance of benthic oxygen supply and demand Marine Ecology Progress Series 155:147-157.

Fox, W. 1988. Modeling of particulate deposition under salmon net pens. Prepared for Washington Dept. of Fisheries by Parametrix, Inc. Bellevue, WA. (appendix to state PEIS)

Franks, J.S., J.R. Warren and M.V. Buchanan. 1999. Age and growth of cobia, *Rachycentron canadum*, from the northeastern Gulf of Mexico. Fish. Bull. 97:459–471.

Fujii, M. S. Murashige, Y. Ohnishi, A. Yuzawa, H. Miyasaka, Y. Suzuki and H. Komiyama. 2002. Decomposition of Phytoplankton in Seawater. Part I: Kinetic Analysis of the Effect of Organic Matter Concentration Journal of Oceanography. 58: 433-438.

Hargrave, B. 1994. Modeling benthic impacts of organic enrichment from marine aquaculture. Canadian Technical Report of Fisheries and Aquatic Sciences 1949. Fisheries and Ocean Canada.

Hendrichs, S.M. and A.P. Doyle. 1986. Decomposition of 14C-labeled organic substances in marine sediments. Limnology and Oceanography. Vol. 31, pp. 765-778.

Ikura, T., 1974. Sinking velocity of faecal pellet and left over food around yellowtail aquaculture. Suisan Zoshoku 22, 34– 39 (inJapanese with English abstract).

Kiefer, D.A. and C.A. Atkinson. 1988. The calculated response of phytoplankton to nutrient loading by Dungeness Bay Sea Farm. Prepared for Sea Farm Washington and the Jamestown S'Klallam Tribe and presented to the Washington State Shorelines Hearing Board.

Kiefer, D.A., and C.A. Atkinson. 1984. Cycling of nitrogen by plankton: a hypothetical description based upon efficiency of energy conversion. J. Marine Research. 42: 655-675.

Kiefer, D.A. and C.A. Atkinson. 1989. The calculated response of phytoplankton in south Puget Sound to nutrient loading by the Swecker Sea Farm. Prepared for Swecker Sea Farm (Rochester Washington) and presented to the Washington State Shorelines Hearing Board. 28 pp.

Liao, I.C. et al. 2004 Cobia culture in Taiwan: current status and problems. Aquaculture 237:155-165.

Magill, S.H,, H. Thetmeyer and C.J. Cromey. In press. Settling velocity of faecal pellets of gilthead sea bream (*Sparus aurata* L.) and sea bass (*Dicentrarchus labrax* L.) and sensitivity analysis using measured data in a deposition model. Aquaculture.

Mercado, A.M., J.E. Capella, J. Corredor and J. Morell (1996) Oceanographic conditions at Vieques Island, P.R., potential OTEC site off Punta Vaca for April and September, 1996. Report prepared at the Department of Marine Sciences, University of Puerto Rico, under contract to Ocean Energy Resources, San Juan, PR, 82 pp.

Morelock, J., Winget, E. A., & Goenaga, C. (1994). Geologic maps of the Puerto Rico insular shelf, Parguera to Guanica. U.S. Geological Survey Misc. Investigations Map I-2387, scale 1:40,000.

Normandeau Associates and Battelle. 2003. Maine Aquaculture Review. Prepared for Maine Department of Marine Resources. Report R-19336.West Boothbay Harbor, Me, 54 pp. http://mainegov-images.informe.org/dmr/aquaculture/reports/MaineAquacultureReview.pdf

Ostrowski, A.C., J. Bailey-Brock and P. Leung. 2001. Hawaii offshore aquaculture research project (HOARP). Submitted to C.E. Helsley, Hawaii Sea Grant. University of Hawaii at Manoa and Oceanic Institute, Oahu, Hawaii. 78 pp.

Panchang, V., G. Cheng, and C.R. Newell. 1997. Modeling hydrodynamics and aquaculture waste transport in coastal Maine. Estuaries 20: 14–41.

Parametrix. 1990. Final programmatic environmental impact statement fish culture in floating net-pens. Prepared by Parametrix Inc, Rensel Associates and Aquametrix Inc. for Washington State Department of Fisheries, 115 General Administration Building, Olympia, WA 98504, 161 p.

Rensel, J.E. 1987. Aquatic conditions at a proposed net-pen site in Northwest Discovery Bay, Washington. Milner-Rensel Associates for Jamestown S'Klallam Tribe and Sea Farm of Norway, Inc. 74 pp and appendices.

Rensel, J.E. 1989a. Phytoplankton and nutrient studies near salmon net-pens at Squaxin Island, Washington. in technical appendices of the State of Washington's Programmatic Environmental Impact Statement: Fish culture in floating net-pens. Washington Department of Fisheries. 312 pp. and appendices.

Rensel, J.E. 1989b. Dissolved nutrients, water quality and phytoplankton studies near the Swecker Sea Farms net-pen site in Lower Case Inlet, and in southern Puget Sound, Washington. Prepared for Swecker Sea Farms, Inc. Tumwater, Washington. 24 pp. plus.

Rensel, J.E., D.A. Kiefer, J.R.M. Forster, D.L. Woodruff and N.R. Evans. In Press a. Offshore finfish mariculture in the Strait of Juan de Fuca. U.S.-Japan Cooperative Program in Natural Resources, 33rd Annual Proceedings. Nagasaki Japan 2004. http://www.wfga.net/sjdf/index.html

Rensel, J.E., A.H. Buschmann, T. Chopin, I.K. Chung, J. Grant, C.E. Helsley, D.A. Kiefer, R. Langan, R.I.E. Newell, M. Rawson, J.W. Sowles, J.P. McVey, and C. Yarish. In press b. Ecosystem based management: Models and mariculture. J.E. Rensel, editor. Pages xx-xx *in* J.P. McVey, C-S. Lee, and P.J. O'Bryen, editors. The Role of Aquaculture in Integrated Coastal and Ocean Management: An Ecosystem Approach. The World Aquaculture Society, Baton Rouge, Louisiana, 70803. United States.

Tlusty, M.F., K Snook, V.A. Pepper and M.R. Anderson. 2000. The potential for soluble and transport loss of particulate aquaculture wastes. Aquaculture Res. 31:745.

Riedel, R. and C. Bridger. 2003. Simulation for Environmental Impact. Mississippi-Alabama Sea Grant Consortium software, Ocean Springs, MS. MASGP-03-001-01.

Westrich, J.T., Berner, R.A., 1984. The role of sedimentary organic matter in bacterial sulphate reduction: the Gmodel tested. Limnol. Oceanogr. 29, 236– 249.

Washington Department of Fisheries. 1991. Programmatic Environmental Impact Statement: Fish culture in floating net-pens. Prepared by Parametrix, Battelle Northwest laboratories and Rensel Associates. Olympia WA. 61 pp.

Wroblewski, J.S., J. L. Sarmiento, and G. R. Flierl. 1988. An Ocean Basin Scale Model of Plankton Dynamics in the North Atlantic 1. Solutions for the Climatological Oceanographic Conditions in May. Global Biogeochemical Cycles, vol. 2(3): 199-218.

12. Appendix A. Sensitivity Analysis Variables

Appendix Table 1. Yellow fill indicates principle variable(s) being varied in each simulation case

Case Number →		**1 Primary**	**2**	**3**	**4**	**5**	**6**	**7**	**8**
Current Velocity	cm s-1	8.4	8.4	8.4	8.4	8.4	8.4	8.4	0.5
Fish Density	kg m-3	15	15	15	7.6	22.6	15	15	30
Fecal Carbon Waste Rate	Percent of food	25	25	25	25	25	25	25	25
Sediment Carbon Oxidation	% per d	1	0.5	1.5	1	1	1	1	1
Fish Size	kg	4.5	4.5	4.5	2.2	4.5	4.5	4.5	4.5
Initial Fish Biomass	MT	413	413	413	209	622	413	413	810
Final Fish Biomass	MT	559	559	559	309	842	559	559	1,118
Feed Rate	% BW per d	4	4	4	4	4	4	4	4
Horizontal Turbulence	unit	0.1	0.1	0.1	0.1	0.1	0.2	0.05	0.1
Vertical Turbulence	unit	0.05	0.05	0.05	0.05	0.05	0.05	0.05	0.05
Resuspension (Erosion) rate	cm s^{-1}	6.0	6.0	6.0	6.0	6.0	6.0	6.0	6.0
Deposition Threshold	cm s^{-1}	4.5	4.5	4.5	4.5	4.5	4.5	4.5	4.5
Ambient Nitrogen	uM	0.15	0.15	0.15	0.15	0.15	0.15	0.15	0.10
Ambient Phytoplankton	ug/L	0.10	0.10	0.10	0.10	0.10	0.10	0.10	0.10
Ambient Zooplankton	ug/L	0.05	0.05	0.05	0.05	0.05	0.05	0.05	0.05

Case Number →		9	10	11	12	13	14	15
Current Velocity	cm s^{-1}	8.4	8.4	8.4	8.4	0.5	8.4	0.5
Fish Density	kg m-3	15	15	15	15	30	15	30
Fecal Carbon Waste Rate	Percent of food	35	25	25	25	25	25	25
Sediment Carbon Oxidation Rate	% per d	1	1	1	1	1	1	1
Fish Size	kg	4.5	4.5	4.5	4.5	4.5	4.5	4.5
Initial Fish Biomass	MT	413	413	413	413	810	413	810
Final Fish Biomass	MT	559	559	559	559	1,118	559	1,118
Feed Rate	% BW per d	4	4	4	4	4	2	4
Horizontal Turbulence	unit	0.1	0.1	0.1	0.1	0.1	0.1	0.1
Vertical Turbulence	unit	0.05	0.05	0.05	0.05	0.05	0.05	0.05
Resuspension (Erosion) rate	cm s^{-1}	6.0	9.5	7.7	6.0	6.0	6.0	6.0
Deposition Threshold	cm s^{-1}	4.5	4.5	4.5	3.0	4.5	4.5	4.5
Ambient Nitrogen	uM	0.15	0.15	0.15	0.15	0.10	0.15	0.15
Ambient Phytoplankton	ug/L	0.10	0.10	0.10	0.10	0.10	0.10	0.10
Ambient Zooplankton	ug/L	0.05	0.05	0.05	0.05	0.02	0.05	0.00

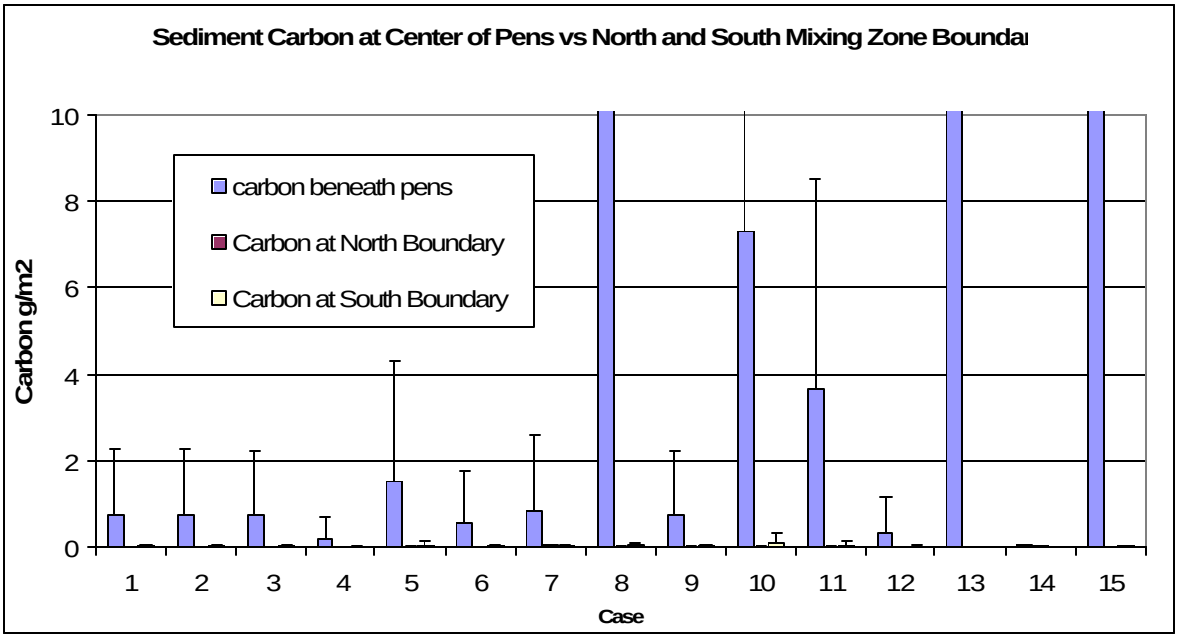

Cases 8, 13 and 15 extend above scale, see appendix table below for results. Data are mean values with 1 standard deviation unit as error bars.

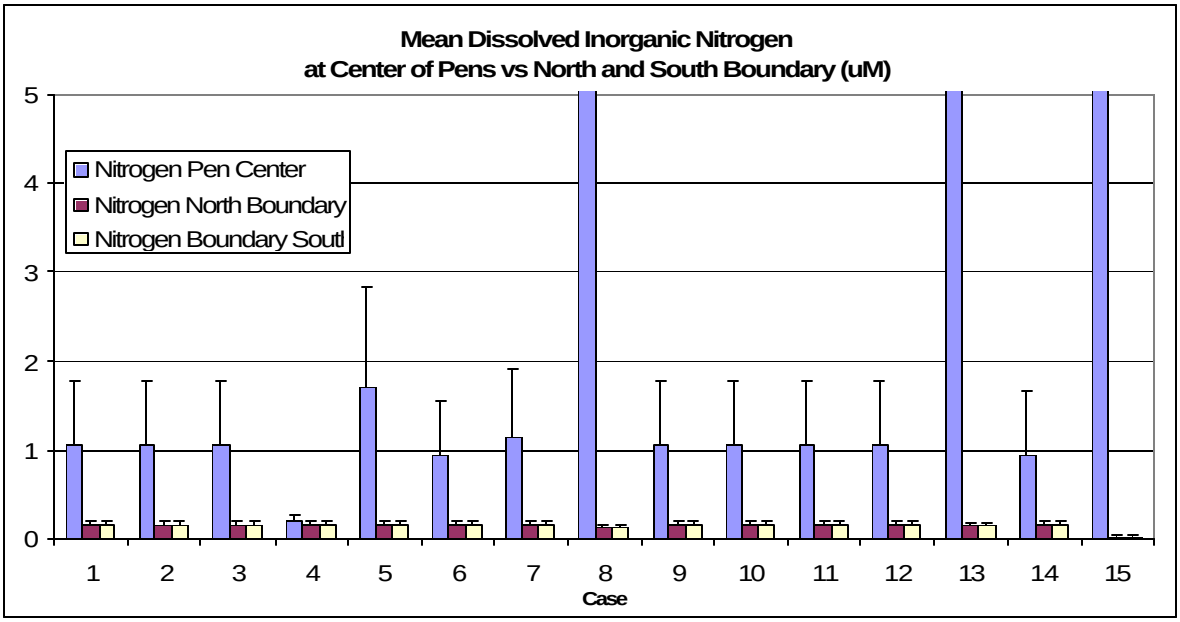

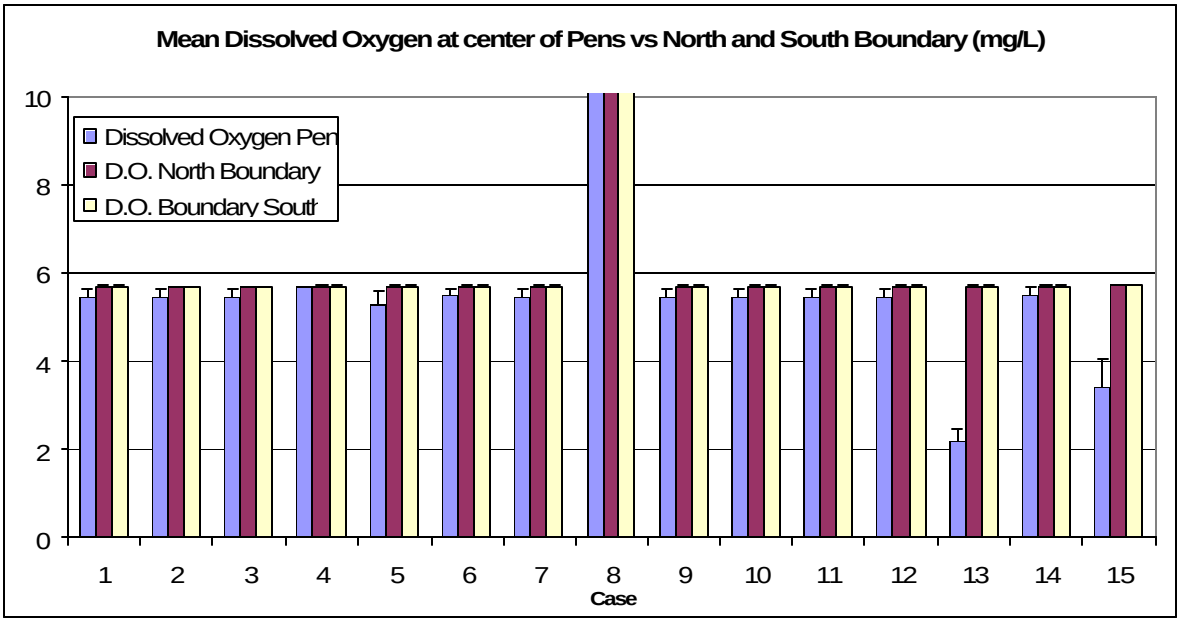

Case 8 was to evaluate bloom potential was set up with very high DO inside cages as an initial condition to allow the higher biomass of fish to respire without constraint. Case 13 was also set up to evaluate bloom conditions but initial D.O. in the cages was not elevated at the start.

Appendix Table 2 (Part 1). Mean, standard deviation, 90th and 10th percentile values for 15 different model run cases. Part 1 shows velocity, fish biomass and south mixing zone boundary results. DIN = dissolved inorganic nitrogen. All parameters are water column measures except sediment carbon. "C" = carbon.

	No.	Flow Velocity	Fish Bio-mass	Dissolved Oxygen South	DIN South	Phyto-plankton South	Zoo-plankton South	Fecal Waste C South	Feed Waste C South	Sedi-ment C South	Dissolved Oxygen North
		cm s^{-1}	MT	mg L^{-1}	µM	µg L^{-1}	µg L^{-1}	g m^{-3}	g m^{-3}	g m^{-2}	mg L^{-1}
Mean	1	8.44	484	5.70	0.16	0.06	0.09	0.00	0.00	0.02	5.70
SD		5.25	42	0.01	0.03	0.03	0.02	0.00	0.00	0.05	0.01
90th %		15.94	543	5.71	0.19	0.10	0.13	0.00	0.00	0.09	5.71
10th %		2.95	426	5.69	0.10	0.03	0.06	0.00	0.00	0.00	5.69
Mean	2	8.44	484	5.69	0.15	0.06	0.09	0.00	0.00	0.02	5.69
SD		5.25	42	0.01	0.04	0.03	0.03	0.00	0.00	0.05	0.01
90th %		15.94	543	5.71	0.20	0.09	0.14	0.00	0.00	0.09	5.71
10th %		2.95	426	5.67	0.07	0.03	0.06	0.00	0.00	0.00	5.67
Mean	3	8.44	490	5.69	0.15	0.06	0.09	0.00	0.00	0.02	5.69
SD		5.25	46	0.01	0.04	0.03	0.03	0.00	0.00	0.05	0.01
90th %		15.94	555	5.71	0.20	0.09	0.13	0.00	0.00	0.09	5.71
10th %		2.95	427	5.68	0.08	0.03	0.06	0.00	0.00	0.00	5.68
Mean	4	8.44	257	5.70	0.16	0.06	0.09	0.00	0.00	0.01	5.70
SD		5.25	29	0.01	0.03	0.03	0.02	0.00	0.00	0.02	0.01
90th %		15.94	298	5.71	0.19	0.10	0.13	0.00	0.00	0.04	5.71
10th %		2.95	218	5.69	0.10	0.03	0.06	0.00	0.00	0.00	5.69
Mean	5	8.44	729	5.70	0.16	0.06	0.09	0.00	0.00	0.04	5.70
SD		5.25	64	0.01	0.03	0.03	0.02	0.00	0.00	0.09	0.01
90th %		15.94	818	5.71	0.19	0.10	0.13	0.00	0.00	0.16	5.71
10th %		2.95	642	5.69	0.10	0.03	0.06	0.00	0.00	0.00	5.69
Mean	6	8.44	484	5.70	0.16	0.06	0.09	0.00	0.00	0.02	5.70
SD		5.25	42	0.01	0.03	0.03	0.02	0.00	0.00	0.04	0.01
90th %		15.94	543	5.71	0.19	0.10	0.13	0.00	0.00	0.08	5.71
10th %		2.95	426	5.69	0.10	0.03	0.06	0.00	0.00	0.00	5.69
Mean	7	8.44	484	5.70	0.16	0.06	0.09	0.00	0.00	0.03	5.70
SD		5.25	42	0.01	0.03	0.03	0.02	0.00	0.00	0.06	0.01
90th %		15.94	543	5.71	0.19	0.10	0.13	0.00	0.00	0.11	5.71
10th %		2.95	426	5.69	0.10	0.03	0.06	0.00	0.00	0.00	5.69
Mean	8	0.50	992	19.99	0.13	0.08	0.08	0.00	0.00	0.07	19.99
SD		0.35	71	0.00	0.02	0.01	0.01	0.00	0.00	0.03	0.00

	No.	Flow Velocity	Fish Bio-mass	Dissolved Oxygen South	DIN South	Phyto-plankton South	Zoo-plankton South	Fecal Waste C South	Feed Waste C South	Sedi-ment C South	Dissolved Oxygen North
		cm s^{-1}	MT	mg L^{-1}	µM	µg L^{-1}	µg L^{-1}	g m^{--3}	g m^{--3}	g m^{-2}	mg L^{-1}
90th %		0.97	1,092	20.00	0.15	0.10	0.10	0.00	0.00	0.11	20.00
10th %		0.03	895	19.99	0.11	0.07	0.07	0.00	0.00	0.03	19.99
Mean	9	8.47	489	5.70	0.15	0.06	0.09	0.00	0.00	0.02	5.70
SD		5.18	46	0.01	0.03	0.03	0.02	0.00	0.00	0.05	0.01
90th %		15.85	554	5.71	0.19	0.10	0.12	0.00	0.00	0.09	5.71
10th %		3.01	427	5.69	0.10	0.03	0.06	0.00	0.00	0.00	5.69
Mean	10	8.44	484	5.70	0.16	0.06	0.09	0.00	0.00	0.11	5.70
SD		5.25	42	0.01	0.03	0.03	0.02	0.00	0.00	0.19	0.01
90th %		15.94	543	5.71	0.19	0.10	0.13	0.00	0.00	0.39	5.71
10th %		2.95	426	5.69	0.10	0.03	0.06	0.00	0.00	0.00	5.69
Mean	11	8.44	484	5.70	0.16	0.06	0.09	0.00	0.00	0.05	5.70
SD		5.25	42	0.01	0.03	0.03	0.02	0.00	0.00	0.08	0.01
90th %		15.94	543	5.71	0.19	0.10	0.13	0.00	0.00	0.19	5.71
10th %		2.95	426	5.69	0.10	0.03	0.06	0.00	0.00	0.00	5.69
Mean	12	8.44	484	5.70	0.16	0.06	0.09	0.00	0.00	0.01	5.70
SD		5.25	42	0.01	0.03	0.03	0.02	0.00	0.00	0.04	0.01
90th %		15.94	543	5.71	0.19	0.10	0.13	0.00	0.00	0.05	5.71
10th %		2.95	426	5.69	0.10	0.03	0.06	0.00	0.00	0.00	5.69
Mean	13	0.12	567	5.70	0.15	0.06	0.09	0.00	0.00	0.00	5.70
SD		0.09	9	0.01	0.03	0.03	0.02	0.00	0.00	0.00	0.01
90th %		0.24	579	5.71	0.19	0.10	0.13	0.00	0.00	0.00	5.71
10th %		0.01	554	5.69	0.09	0.03	0.06	0.00	0.00	0.00	5.69
Mean	14	8.44	481	5.70	0.16	0.06	0.09	0.00	0.00	0.00	5.70
SD		5.25	41	0.01	0.03	0.03	0.02	0.00	0.00	0.01	0.01
90th %		15.94	540	5.71	0.19	0.10	0.13	0.00	0.00	0.02	5.71
10th %		2.95	426	5.69	0.10	0.03	0.06	0.00	0.00	0.00	5.69
Mean	15	0.50	466	5.74	0.01	0.24	0.00	0.00	0.00	0.02	5.74
SD		0.35	31	0.01	0.02	0.02	0.00	0.00	0.00	0.01	0.01
90th %		0.97	510	5.74	0.01	0.25	0.00	0.00	0.00	0.04	5.74
10th %		0.03	424	5.74	0.00	0.24	0.00	0.00	0.00	0.00	5.74

Part 2. North mixing zone boundary and Net pen location results, north mixing zone boundary fecal and feed wastes column omitted as they were all zeros.

	No.	DIN North	Phyto-plankton North	Zoo-plankton North	Sediment Carbon North	Oxygen Pen Center	DIN Pen Center	Phyto-plankton Pen	Zoo-plankton Pen	Fecal Waste C Pen	Feed Waste C Pen	Sediment C Pen
		µM	µg L^{-1}	µg L^{-1}	g m^{-2}	mg L^{-1}	µM	µg L^{-1}	µg/L	g m^{--3}	g m^{-3}	g m^{-2}
Mean	1	0.16	0.06	0.09	0.00	5.47	1.06	0.06	0.09	0.02	0.06	0.75
SD		0.03	0.03	0.02	0.01	0.18	0.71	0.03	0.02	0.04	0.03	1.51
90th%		0.19	0.10	0.13	0.00	5.63	1.96	0.10	0.13	0.03	0.10	2.82
10th%		0.10	0.03	0.06	0.00	5.24	0.42	0.03	0.06	0.01	0.03	0.00
Mean	2	0.15	0.06	0.09	0.00	5.45	1.06	0.06	0.09	0.01	0.04	0.75
SD		0.04	0.03	0.03	0.01	0.18	0.72	0.03	0.03	0.03	0.01	1.51
90th%		0.20	0.09	0.14	0.00	5.62	1.96	0.09	0.14	0.02	0.06	2.84
10th%		0.07	0.03	0.06	0.00	5.22	0.42	0.03	0.06	0.01	0.02	0.00
Mean	3	0.15	0.06	0.09	0.00	5.46	1.05	0.06	0.09	0.01	0.04	0.69
SD		0.04	0.03	0.03	0.01	0.18	0.70	0.03	0.03	0.04	0.01	1.45
90th%		0.20	0.09	0.13	0.00	5.62	1.93	0.09	0.13	0.02	0.06	2.69
10th%		0.08	0.03	0.06	0.00	5.23	0.43	0.03	0.06	0.01	0.02	0.00
Mean	4	0.16	0.06	0.09	0.00	5.68	0.21	0.06	0.09	0.01	0.02	0.21
SD		0.03	0.03	0.02	0.01	0.01	0.04	0.03	0.02	0.02	0.01	0.51
90th%		0.19	0.10	0.13	0.00	5.70	0.25	0.10	0.13	0.02	0.04	0.62
10th%		0.10	0.03	0.06	0.00	5.67	0.15	0.03	0.06	0.01	0.01	0.00
Mean	5	0.16	0.06	0.09	0.00	5.30	1.70	0.06	0.09	0.03	0.09	1.52
SD		0.03	0.03	0.02	0.02	0.29	1.14	0.03	0.02	0.06	0.04	2.78
90th%		0.19	0.10	0.13	0.00	5.57	3.16	0.10	0.13	0.04	0.15	6.21
10th%		0.10	0.03	0.06	0.00	4.93	0.66	0.03	0.06	0.01	0.04	0.00
Mean	6	0.16	0.06	0.09	0.00	5.50	0.94	0.06	0.09	0.02	0.06	0.57
SD		0.03	0.03	0.02	0.01	0.16	0.62	0.03	0.02	0.04	0.03	1.20
90th%		0.19	0.10	0.13	0.00	5.64	1.70	0.10	0.13	0.02	0.09	2.03
10th%		0.10	0.03	0.06	0.00	5.30	0.38	0.03	0.06	0.01	0.03	0.00
Mean	7	0.16	0.06	0.09	0.00	5.45	1.15	0.06	0.09	0.02	0.06	0.86
SD		0.03	0.03	0.02	0.01	0.20	0.77	0.03	0.02	0.01	0.03	1.72
90th%		0.19	0.10	0.13	0.00	5.63	2.12	0.10	0.13	0.03	0.10	3.36
10th%		0.10	0.03	0.06	0.00	5.19	0.44	0.03	0.06	0.01	0.03	0.00
Mean	8	0.13	0.08	0.08	0.07	14.21	22.71	0.10	0.08	0.07	0.28	701.45

	No.	DIN North	Phyto-plankton North	Zoo-plankton North	Sediment Carbon North	Oxygen Pen Center	DIN Pen Center	Phyto-plankton Pen	Zoo-plankton Pen	Fecal Waste C Pen	Feed Waste C Pen	Sediment C Pen
		µM	µg L^{-1}	µg L^{-1}	g m^{-2}	mg L^{-1}	µM	µg L^{-1}	µg/L	g m^{--3}	g m^{-3}	g m^{-2}
SD		0.02	0.01	0.01	0.03	1.91	7.44	0.01	0.02	0.01	0.04	289.86
90th%		0.15	0.10	0.10	0.11	16.32	34.06	0.11	0.10	0.08	0.33	1107.28
10th%		0.11	0.07	0.07	0.03	11.31	14.49	0.08	0.07	0.06	0.23	304.46
Mean	9	0.15	0.06	0.09	0.00	5.47	1.06	0.06	0.09	0.02	0.04	0.70
SD		0.03	0.03	0.02	0.01	0.18	0.70	0.03	0.02	0.01	0.01	1.46
90th%		0.19	0.10	0.12	0.00	5.63	1.94	0.10	0.12	0.03	0.05	2.72
10th%		0.10	0.03	0.06	0.00	5.24	0.43	0.03	0.06	0.01	0.02	0.00
Mean	10	0.16	0.06	0.09	0.02	5.47	1.06	0.06	0.09	0.02	0.06	7.30
SD		0.03	0.03	0.02	0.04	0.18	0.71	0.03	0.02	0.01	0.03	9.32
90th%		0.19	0.10	0.13	0.08	5.63	1.96	0.10	0.13	0.03	0.10	24.40
10th%		0.10	0.03	0.06	0.00	5.24	0.42	0.03	0.06	0.01	0.03	0.00
Mean	11	0.16	0.06	0.09	0.01	5.47	1.06	0.06	0.09	0.02	0.06	3.64
SD		0.03	0.03	0.02	0.02	0.18	0.71	0.03	0.02	0.01	0.03	4.89
90th%		0.19	0.10	0.13	0.02	5.63	1.96	0.10	0.13	0.03	0.10	12.63
10th%		0.10	0.03	0.06	0.00	5.24	0.42	0.03	0.06	0.01	0.03	0.00
Mean	12	0.16	0.06	0.09	0.00	5.47	1.06	0.06	0.09	0.02	0.06	0.34
SD		0.03	0.03	0.02	0.01	0.18	0.71	0.03	0.02	0.01	0.03	0.80
90th%		0.19	0.10	0.13	0.00	5.63	1.96	0.10	0.13	0.03	0.10	1.22
10th%		0.10	0.03	0.06	0.00	5.24	0.42	0.03	0.06	0.01	0.03	0.00
Mean	13	0.15	0.06	0.09	0.00	2.20	13.83	0.05	0.09	0.01	0.33	704.43
SD		0.03	0.03	0.02	0.03	0.30	1.08	0.02	0.02	0.05	0.03	390.24
90th%		0.19	0.10	0.13	0.00	2.53	15.23	0.10	0.13	0.01	0.37	1233.72
10th%		0.09	0.03	0.06	0.00	1.84	12.55	0.03	0.07	0.00	0.29	153.02
Mean	14	0.16	0.06	0.09	0.00	5.50	0.93	0.06	0.09	0.02	0.00	0.07
SD		0.03	0.03	0.02	0.00	0.19	0.75	0.03	0.02	0.01	0.00	0.19
90th%		0.19	0.10	0.13	0.00	5.69	1.85	0.10	0.13	0.03	0.00	0.22
10th%		0.10	0.03	0.06	0.00	5.26	0.17	0.03	0.06	0.01	0.00	0.00
Mean	15	0.01	0.24	0.00	0.02	3.41	9.11	0.24	0.00	0.03	0.17	355.85
SD		0.02	0.02	0.00	0.01	0.66	2.57	0.02	0.00	0.05	0.05	204.18
90th%		0.01	0.25	0.00	0.04	4.23	12.74	0.25	0.00	0.03	0.25	640.46
10th%		0.00	0.24	0.00	0.00	2.48	5.91	0.25	0.00	0.01	0.11	75.33

13. Appendix B. Modeling Team Background

1) Dr. Rensel has over 30 years experience in benthic ecology and fish farm impacts since the first study of fish mariculture impacts in Puget Sound. He conducts routine monitoring for NPDES compliance and research at several net pen facilities in Puget Sound and helped design State of Washington performance standards by working with State government and industry. He has been a contributor to phytoplankton studies worldwide including harmful algae, effects on fish and shellfish and mitigation means.
2) Mr. O'Brien is a highly experienced modeler and software engineer. He wrote much of the underlying code for EASy and developed the Mariculture module.
3) Dr. Kiefer is also an experienced modeler with extensive experience in phytoplankton dynamics and physiology and has been active for several years in fish farm effects modeling and studies as described in Section D above.

Short version of resumes follow:

J.E. Jack Rensel, Principal Investigator, Senior Scientist, System Science Applications

Ph.D. Fisheries and Oceanography, University of Washington, Seattle, WA
M.S. University of Washington, Seattle & Stanford University Hopkins Marine Station, Pacific Grove CA
B.S. Western Washington University, Bellingham, WA

Dr. Jack Rensel is a senior scientist with SSA and has conducted over a dozen siting and impact assessments for fish mariculture in the U.S. during the period 1980-90. Many site-specific studies were conducted after site establishment to measure performance relative to standards. After helping the State of Washington design fish farming performance standards and monitoring protocols, he served as national co-chair of the Joint Subcommittee on Aquaculture (USDA) technical net pen committee to work with U.S. EPA on their performance standard development. He previously served as primary participant in the 12-year research and rule making process for cage mariculture in Puget Sound with the Washington Department of Ecology. He recently led NOAA's efforts to organize and conduct part of an international workshop on coastal mariculture with his session focusing on modeling. Rensel is presently examining the beneficial effects of marine finfish mariculture in Puget Sound with regard to biofouling.

He has been involved in fish culture since conducting the first impact studies of fish rearing on the benthic environment in Puget Sound in 1972. Subsequently he was responsible for managing and expanding one of the world's largest public-owned net pen enhancement facilities (Squaxin Island), which included a five-year tagging and fisheries contribution published study (Rensel et al. 1988). Since 1983 he has consulted for leading fish farming companies and government agencies, here and abroad for site studies, benthic and water column impact assessment and harmful algal bloom management and monitoring studies. His experience includes dozens of circulation studies, hatchery impact studies, pesticide and nutrient monitoring efforts and related work. Presently Dr. Rensel is completing extensive studies of the dynamics of invertebrate and plant colonization of fish farm substrates.

Selected Publications (see literature cited for most recent) plus:

Rensel, J.E., D.A. Kiefer, J.R.M. Forster, D.L. Woodruff and N.R. Evans. In Press. **Offshore finfish mariculture in the Strait of Juan de Fuca.** U.S.-Japan Cooperative Program in Natural Resources, 33rd Annual Proceedings. Nagasaki Japan 2004. See http://www.wfga.net/sjdf/reports/publication.pdf

Rensel, J. E. and J.N.C. Whyte. 2003. **Finfish mariculture and Harmful Algal Blooms** . Second Edition. pp. 693-722 In: UNESCO Manual on Harmful Marine Microalgae. D. Anderson, G. Hallegaeff and A. Cembella (eds). IOC monograph on Oceanographic Methodology. http://upo.unesco.org/bookdetails.asp?id=4040

Rensel, J.E. 2003. **Dungeness Bay Bathymetry, Circulation and Fecal Coliform Studies. Phase 2.** Prepared by Rensel Associates Aquatic Science Consultants, Arlington, Washington for the Jamestown S'Klallam Tribe, Sequim Washington and the U.S. Environmental Protection Agency, Seattle, Washington. 94 p. http://www.jamestowntribe.org/Dungeness%20Bay%20Final%20report%20P2,%2014%20Apr%2003.pdf

Anderson, D.M., P. Andersen, V.M. Bricelj, J.J. Cullen, and J.E. Rensel. 2001. **Monitoring and Management Strategies for Harmful Algal Blooms in Coastal Waters,** APEC #201-MR-01.1, Asia Pacific Economic Program, Singapore, and Intergovernmental Oceanographic Commission Technical Series No. 59, Paris. 264 p. http://www.whoi.edu/redtide/Monitoring_Mgt_Report.html

Rensel, J.E. 2001. **Salmon net pens in Puget Sound: Rules, performance criteria and monitoring**. Global Aqua.Adv. 4(1):66-69.

Rensel, J.E. 1993. **Factors controlling Paralytic Shellfish Poisoning in Puget Sound**. Journal of Shellfish Research 12:2:371-376.

Rensel Associates and PTI Environmental Services. 1991**. Nutrients and Phytoplankton in Puget Sound**. Prepared for US Environmental Protection Agency Report 910/9-91-002. Seattle.130 pp.

Rensel, J.E. 1993. **Severe blood hypoxia of Atlantic salmon (*Salmo salar*) exposed to the marine diatom *Chaetoceros concavicornis.*** pp. 625-630. In: Toxic Phytoplankton Blooms in the Sea. T.J. Smayda and Y. Shimizu (eds). Elsevier Science Publishers B.V., Amsterdam

Rensel Associates and PTI Environmental Services. 1991. **Nutrients and Phytoplankton in Puget Sound**. Peer reviewed monograph prepared for U.S. EPA, region X, Seattle. Report 910/9-91-002. 130 pp.

Frank O'Brien, Systems Engineer, System Science Application

Professional Preparation

University of Vermont, Burlington, VT	Mathematics	B.A.	1965
University of Vermont, Burlington, VT	Mathematics	M.A.	1967
Cal State University, Fullerton, CA	MBA (33 credits towards)		

Advanced Technical Training in DCOM, MTS, MSMQ, OLEDB, C#, and DotNet

Appointments

Director of Software Engineering, System Science Applications, CA. 2001-2006
Systems Engineering Lead, Logicon, Inc., San Pedro, CA. 1988-2001
Division Manager, Comarco Inc., Anaheim CA. 1981-1988
Program Development Manager, Logicon, Inc., San Pedro, CA. 1972-1980
Programmer, North American Rockwell, Anaheim, CA. 1969-1972.

Computer Experience

Machines: PC (26 years), Sun (years1), DEC (2years), IBM mainframes (15 years)
Operating Systems: Windows XP, 2000, NT, 98, 95, 3.1 (11 years), UNIX (1 year), DOS (22 y.)
Languages:VC++ (14 years), VB (9 years), Java (7 year), Assembler (22 years), Fortran (30 years)
Technologies: COM (8 years); ODBC, DAO (8 years); MTS, MSMQ, ADO, OLE-DB (7 years)

Extensive experience in every Phase of software development including management and business development, requirements analysis, algorithm development, and prototyping.

Synergistic Activities

- Architect and lead developer of EASy GIS software, a dynamic 3D oceanographic GIS system, and its NetViewer GIS web-server component.
- Programming for the development of a series of information systems in support of mariculture environmental analysis, fisheries management, fish tracking, marine biogeographical, hydro-optical water analysis, water quality studies, and coastal area management projects including the Gulf of Maine Biogeographic Information System (Sloan/NOPP), NOAA-NESDIS Sea Nettles, Santa Monica Bay Virtual Ocean (SMBRP).

List of Collaborators last 48 Months

M. Domeier, PIER Institute
P. Cornillon, University of Rhode Island
R. Branton, Bedford Institute of Oceanography
B. White, LA Department of Water & Power
M. Yamaguchi, Santa Monica Bay Restoration Project
C. Brown, NOAA/NESDIS
J. Latham, SDRN, FAO-United Nations
D. Foley, NOAA/NMFS NWFSC

Dale A. Kiefer, President & Chief Scientist, System Science Applications

Professional Preparation

Yale University	Biology		B.Sc.	1966
University of Oregon	Marine Biology		M.S.	1967
UC San Diego (Scripps)	Biological Oceanography	Ph.D.	1973	

Appointments

Professor, Department of Biological Sciences, University of Southern California, 1990-
SeaWiFS Science Team, NASA, 1993-
Visiting Scientist, Food and Agricultural Organization, United Nations, Rome, Italy 1994-98
Visiting Scientist, Laboratoire de Pierre et Marie Curie, University of Paris, France, 1987
Associate Professor, Department of Biological Sciences, Univ. of Southern California, 1981-90
Assistant Professor, Department of Biological Sciences, Univ. of Southern California, 1976-81
Assistant Research Biologist, U.C. San Diego Visibility Laboratory, 1975-76.

Short Resume: Dr. Kiefer, after working as a researcher for the Scripps' Marine Life Research Group and Visibility Laboratory, joined the faculty at the University of Southern California and is now a full

professor in the Department of Biological Sciences. His research, which has been funded by numerous government agencies including NSF, the NASA, NOAA, and ONR, has received international recognition. As a member of NASA's SeaWiFS Science Team he has worked to develop algorithms for the mapping of photosynthesis and bio-optical properties from satellite ocean color imagery. In 1995 he served for 2 years as consultant to the UN-FAO in Rome, Italy, where he applied his expertise in remote sensing to fishery management. He is a member of the Heinz Foundation's State of the Ecosystem Panel for coastal waters. Kiefer has published 75 papers and 16 published reports, 47 in the field of bio-optical oceanography, 21 relating to phytoplankton dynamics and modeling, 8 on pollution/water quality issues including aquaculture, and 8 on fisheries/information systems. He has obtained 3 United States patents for inventions in optical instrumentation and wave damping floats.

He is also Chief Scientist and co-founder of System Science Applications, and has supervised the development of several federally funded environmental analysis systems. Examples include the Gulf of Maine Biogeographic Information System and The Gulf of Maine Dynamic Atlas (NOPP),, the Application of Remote Sensing Data to the Analysis of Environmentally-mediated Recruitment Variability in Harvested Fish Populations: Case study of Cod and Haddock Stocks within the Gulf of Maine (NOAA). One program, called the Hydro-Optical Analysis System (HOPAS), is currently being developed on a NSF-sponsored SBIR project for which he served as the Phases I and II Principal Investigator while at System Science Applications. He has modeled and analyzed ocean pollution problems involving fish farm operations, pulp mill and power plant waste water discharges, and offshore waste incineration. He has developed simulation models of fish populations and plankton ecosystem dynamics, and performed studies involving ocean optics, bioluminescence, and air-sea gas exchange.

Selected Publications and Reports:

1995. Ondercin, D., C. A. Atkinson, and D. A. Kiefer. The distribution of bioluminescence and chlorophyll during the late summer in the North Atlantic: maps and a predictive model. Journal of Geophysical Research, 100:6575-6590.

1984. Kiefer, D.A., and C.A. Atkinson. Cycling of nitrogen by plankton: a hypothetical description based upon efficiency of energy conversion. J.Marine Research. 42:655-675.